CALIFORNIA INSTITUTE OF TECHNOLOGY

# I

# CONDITIONS AT A REVERSE-BIASED p-n JUNCTION IN THE PRESENCE OF COLLECTED CURRENT

# II

# EFFECTS OF MODIFIED COLLECTOR BOUNDARY CONDITIONS ON THE BASIC PROPERTIES OF A TRANSISTOR

by
R. D. Middlebrook

Solid State Electronics Laboratory

January 1963

# CONDITIONS AT A REVERSE-BIASED p-n JUNCTION IN THE PRESENCE OF COLLECTED CURRENT

R. D. Middlebrook

Department of Engineering and Applied Science

California Institute of Technology

Pasadena, California

Abstract

An abrupt p-n junction, such as occurs at the collector junction of an n-p-n transistor, is considered. The ratio of n- to p-region conductivity is taken to be very high, so that the transition region is restricted almost entirely to the p-region. The electron density distribution $n$ within the transition region is investigated as a function of the applied reverse bias $V_c$, and of the minority carrier electron current density $J$ which is injected into the transition region from the neutral p-region. It is shown that significant departures occur from the conventional solutions in which the presence of current is neglected. In particular, the electron density $n_c$ at the plane of injection and the transition region thickness $w_t$, used as collector boundary conditions in the analysis of transistor operation, are shown to be current-dependent.

Two cases are considered. In Case I, applicable to transistors with an epitaxial layer under the collector, the electron velocity is assumed much less than the limiting drift velocity. For low injection level, where the minority carrier density $n$ is everywhere less than the equilibrium majority carrier density $p_p$, the transition region is essentially a depletion region and the injected electrons move in an electric field determined uniquely by the applied voltage. It is shown that $n_c \propto J$ and $w_t \propto V_c^{1/2}$. For high injection level, when $n \gg p_p$, the transition region is essentially an accumulation region, and conditions of space-charge-limited current flow are established for which $n_c \propto J^{2/3}$ and $w_t \propto V_c^{2/3}/J^{1/3}$.

In Case II, applicable to most alloy and diffused-base transistors, the electron velocity is assumed equal to the limiting drift velocity

throughout the transition region. Mobile carrier depletion at low injection again gives way to accumulation at high injection. The functional relationships remain as for Case I at low injection, but become $n_c \propto J$, $w_t \propto V_c^{1/2}/J^{1/2}$ at high injection.

Semi-quantitative and detailed quantitative treatments are developed, and normalized graphs of the minority carrier density as a function of distance within the transition region are given for various junction voltages and injected currents.

Contents

## Notation

(Symbols not explicitly defined in the text)

| | |
|---|---|
| $e$ | magnitude of the electronic charge |
| $k$ | Boltzmann's constant |
| $T$ | absolute temperature |
| $\epsilon$ | permittivity |
| $n_n, n_p$ | thermal-equilibrium electron density in the neutral n-region, p-region |
| $p_n, p_p$ | thermal-equilibrium hole density in the neutral n-region, p-region |

## 1. Introduction

In the elementary analysis of a p-n junction, first propounded by Shockley[1] and since extended by many other workers, it is usual to assume that a charge-neutral region is separated from the metallurgical junction by a sharply-defined transition region in which complete charge depletion exists. When the junction current is zero, or very small, use of this model permits simple solutions to be obtained for the transition region thickness in terms of the junction voltage, and for the mobile carrier distributions as functions of distance. In particular, the minority carrier density at the edge of the neutral region is related to its equilibrium value by a Boltzmann factor in the junction voltage, and becomes essentially zero for a reverse bias of more than a few tenths of a volt.

When a reverse-biased p-n junction is employed as a collector in a junction transistor, it is usual to carry over the zero-current solution of the transition region, and to set the minority carrier density equal to zero at the collector edge of the base neutral region as a boundary value in the solution of the differential equation for minority carrier flow. This practice, almost universally accepted, is open to the serious objection that the presence of non-zero collected current would require infinite charge velocity if the density were zero. Since there is a limiting drift velocity for mobile carriers in a solid, this condition clearly cannot exist. Some attention to this problem has been given by Matz[2] and by Kirk.[3]

The purpose of this paper is to investigate the minority carrier density in the vicinity of a reverse-biased collector junction in the

presence of a non-zero collected current. In the light of the above-mentioned objections, the density clearly cannot be zero except at zero current. Two cases are considered.

In Case I, it is assumed that the minority carrier velocity $v$ throughout the collector transition region is less than the limiting drift velocity $v_m$, so that treatment in terms of drift and diffusion currents is valid. This case is applicable to transistors in which there is an epitaxial layer of low conductivity in front of the collector. In Case II, it is assumed that the minority carrier velocity $v$ throughout the collector transition region is equal to the limiting drift velocity $v_m$. This case is applicable to most alloy and diffused-base transistors, and is therefore the one of greatest practical interest. In both cases, the minority carrier density as a function of distance through the transition region is studied.

The non-zero value of the minority carrier density at the edge of the neutral region, in the presence of current, and the current dependence of the transition region thickness, have implications in the elementary analysis of a junction transistor. Some of these effects, incorporated as "modified collector boundary conditions," are studied in a companion paper.[4]

## 2. Case I, $v \ll v_m$: semi-quantitative treatment

An isolated reverse-biased p-n junction is considered in which both the junction voltage and the minority carrier current are taken to be externally-imposed independent variables. Only when the junction

is considered as part of a complete device, such as a transistor, is the current an implicit function of other parameters. A high ratio of n- to p-region conductivity is assumed, and the minority current of interest is electron current injected into the transition region from the neutral p-region. Results of the study of this structure are therefore applicable to the base-collector junction of an n-p-n transistor.

The thickness of the transition region, and the distribution of minority carrier density within it, as functions of the junction voltage and injected minority current, are the quantities of primary interest. In this section a semi-quantitative treatment is presented for Case I, in which the minority carrier velocity within the transition region is everywhere less than the limiting drift velocity.

The discussion is based on the model shown in Fig. 1, and incorporates the following features and assumptions. A p-region of moderate, uniform acceptor doping density $N_A$ forms an abrupt metallurgical junction with an n-region of very high, uniform donor doping density $N_D$. The vertical axis is linear distance increasing upwards, and the horizontal density scale is distorted in order to accommodate orders of magnitude density differences while retaining the qualitative features of a linear scale. A planar junction is assumed. Because of the large ratio $N_D/N_A$, the transition region appears almost entirely within the p-region. When the junction is in thermal equilibrium (zero applied voltage and current), it is well established that the transition region, which is essentially completely depleted of mobile carriers, may be assumed to extend a well-defined distance $w_t$ into the p-region. With

this basic assumption, it is easy to obtain expressions for $w_t$ and the electron density $n$, which in turn can be used to verify the assumption. As a foundation for the later discussion of non-equilibrium conditions, and to introduce the notation, these expressions will be derived.

As indicated in Fig. 1, the origin for distance $x$, potential $V$, and electric field $E = -dV/dx$ within the transition region, is taken at the edge of the neutral p-region. The thermal-equilibrium electron density distribution in the transition region may be obtained by setting the algebraic sum of the drift and diffusion currents equal to zero. This gives

$$e\mu_n nE + eD_n \frac{dn}{dx} = 0 \qquad (1)$$

where the electron diffusion constant $D_n$ and mobility $\mu_n$ are related by $D_n/\mu_n = kT/e \equiv V_t$. With the substitution $E = -dV/dx$, equation (1) may be integrated directly to give $n$ as a function of $V$, where $n = n_n$ when $V = V(w_t)$:

$$n = n_n e^{[V-V(w_t)]/V_t} \qquad (2)$$

Under thermal equilibrium conditions, $n = n_p$ at $x = 0$ and $V(w_t)$ is the internal contact potential $V_i$. Hence from (2),

$$V(w_t) = V_i = V_t \ln(n_n/n_p) \tag{3}$$

The potential $V$ may be found as a function of $x$ from the solution of Poisson's equation. The assumption of complete depletion in the transition region allows the net charge density to be taken as $-eN_A$. Hence Poisson's equation may be written

$$\frac{dE}{dx} = -\frac{eN_A}{\epsilon} \tag{4}$$

It is convenient to introduce the Debye length $L_D$, defined by

$$L_D \equiv \sqrt{\frac{\epsilon V_t}{eN_A}} \tag{5}$$

A typical value at room temperature for p-type germanium of about 2 ohm-cm resistivity is $L_D \approx 10^{-5}$ cm. In terms of the Debye length, Poisson's equation for the transition region becomes

$$\frac{1}{V_t}\frac{dE}{dx} = -\frac{1}{L_D^2} \tag{6}$$

One integration of equation (6) with the boundary condition $E = 0$ at $x = 0$ gives

$$E = - \frac{V_t}{L_D} \frac{x}{L_D} \tag{7}$$

and a second integration with the boundary condition $V = 0$ at $x = 0$ gives

$$V = \frac{V_t}{2} \left( \frac{x}{L_D} \right)^2 \tag{8}$$

Under thermal equilibrium conditions, the voltage change across the whole transition region is the contact potential $V_i$, and so from (8)

$$w_t = \sqrt{2} L_D \left( \frac{V_i}{V_t} \right)^{1/2} \tag{9}$$

A typical value corresponding to $L_D = 10^{-5}$ cm is $w_t \approx 4 \times 10^{-5}$ cm. Substitution of (8) and (9) into (2) gives

$$n = n_n e^{-[1-(V/V_i)]V_i/V_t} = n_n e^{-[1-(x/w_t)^2]V_i/V_t} \tag{10}$$

It is convenient at this stage to convert the various results to normalized form. The normalizing parameters are: density $p_p$, distance $L_D$, and voltage $V_t$. In order that the familiar symbols may be retained, normalized quantities will be distinguished from the originals by use of bold-face type, so that $\underset{\sim}{n} \equiv n/p_p$, $\underset{\sim}{x} \equiv x/L_D$, $\underset{\sim}{V} \equiv V/V_t$, etc. In

normalized form, equations (7) through (10) read

$$E = -\frac{V_t}{L_D}\underset{\sim}{x} \tag{11}$$

$$\underset{\sim}{V} = \frac{1}{2}\underset{\sim}{x}^2 \tag{12}$$

$$\underset{\sim}{w}_t = \sqrt{2}\underset{\sim}{V}_i^{1/2} \tag{13}$$

$$\underset{\sim}{n} = \underset{\sim}{n}_n e^{-[1-(\underset{\sim}{V}/\underset{\sim}{V}_i)]\underset{\sim}{V}_i} = \underset{\sim}{n}_n e^{-[1-(\underset{\sim}{x}/\underset{\sim}{w}_t)^2]\underset{\sim}{V}_i} \tag{14}$$

The conclusion from (14) is that the electron density $\underset{\sim}{n}$ falls off very rapidly from the value $\underset{\sim}{n}_n$ with increasing distance from the metallurgical junction, and is essentially equal to $\underset{\sim}{n}_p = \underset{\sim}{n}_n \exp(-\underset{\sim}{V}_i)$ throughout most of the transition region. A similar argument leads to a corresponding result for the hole density, which falls off very rapidly from its initial value $p_p$ at the edge of the neutral p-region to the value $p_n$ throughout most of the transition region. The initial assumption that the net charge density in the transition region is $-eN_A$ is therefore vindicated except at the extreme edges.

If an external reverse bias $V_c$ is applied across the junction, the above results remain valid if $V_i$ in equations (13) and (14) is replaced by $V_c+V_i \equiv V_{ci}$, as long as the condition of zero current may still be imposed on equation (1). This is not exactly correct, because even if no current is injected from another junction a reverse saturation current

will flow for a finite width of neutral p-region. However, the reverse current will be very small compared with the drift and diffusion components of equation (1). Generation and recombination within the transition region are neglected. Thus in the presence of an externally-applied reverse voltage $V_c$, the transition region thickness becomes

$$\underset{\sim}{w}_t = \sqrt{2}\underset{\sim}{V}_{ci}^{1/2} \tag{15}$$

The electron density distribution is given by

$$\underset{\sim}{n} = \underset{\sim}{n}_n e^{-[1-(\underset{\sim}{V}/\underset{\sim}{V}_{ci})]\underset{\sim}{V}_{ci}} = \underset{\sim}{n}_p e^{\underset{\sim}{V}} \tag{16}$$

and is therefore related to the voltage through a Boltzmann factor. By use of equations (12) and (15), equation (16) can be expressed explicitly in terms of distance:

$$\underset{\sim}{n} = \underset{\sim}{n}_n e^{-[1-(\underset{\sim}{x}/\underset{\sim}{w}_t)^2]\underset{\sim}{V}_{ci}} \tag{17}$$

The electron density, while still reaching $\underset{\sim}{n}_n$ at the metallurgical junction, becomes less than $\underset{\sim}{n}_p$ and essentially equal to $\underset{\sim}{n}_n \exp(-\underset{\sim}{V}_{ci}) = \underset{\sim}{n}_p \exp(-\underset{\sim}{V}_c) \approx 0$ throughout most of the transition region, which itself becomes wider according to equation (15). The model corrected for the presence of the external bias $V_c$ is shown in Fig. 2.

The above conclusions constitute the conventional results for the

reverse-biased collector of an n-p-n transistor, in which the value $\underset{\sim}{n} \approx 0$ at $\underset{\sim}{x} = 0$ is employed as the collector boundary value for the solution of the equation for minority carrier flow in the neutral p-region. Since in normal transistor operation a considerable current may be injected into the neutral p-region from the emitter junction, the previous assumption of negligible collector current is violated. We now wish to remove this restriction from the above analysis.

As already forecast in the Introduction, a non-zero collector boundary value of electron density will be required in the presence of injected current. It is convenient to introduce a special subscript c for the value of n at $x = 0$, so that the collector boundary value is $n_c$, and in normalized form is $\underset{\sim}{n}_c \equiv n_c/p_p$. We consider two conditions. First, we assume that the electron density in the transition region, although no longer zero, is everywhere less than the equilibrium majority carrier density $p_p$. This condition implies $\underset{\sim}{n} \ll 1$, and is defined as "low-level injection." Second, we assume that the electron density in the transition region is everywhere greater than the equilibrium majority carrier density, so that $\underset{\sim}{n} \gg 1$, and this condition is defined as "high-level injection." We consider first, in a semi-quantitative manner, the condition when $\underset{\sim}{n} \ll 1$.

## 2.1. Low-level injection in the transition region; $\underset{\sim}{n} \ll 1$

The problem to be considered is defined as follows. A p-n junction of the type shown in Fig. 1 is subjected to a known reverse voltage bias, and a known current of minority carrier electrons is injected into the

transition region from the neutral p-region. One-dimensional flow is assumed, and generation and recombination are neglected so that the injected current remains constant throughout the transition region. We wish to know the distribution of electron density $n$ in the transition region, and in particular its value $n_c$ at the plane of current injection, since this is the required boundary value for use in analysis of a transistor.

As it is to be assumed first that the electron density in the transition region is everywhere much less than the equilibrium majority carrier density, it follows that the net charge density remains essentially $-eN_A$, and the electric field is therefore the same as in the absence of injected current and is given by equation (11). The transition region thickness is still given by equation (15), and is therefore independent of the injected current. The injected electron current density $j_n$ remains constant throughout the transition region, and is the algebraic sum of drift and diffusion components:

$$e\mu_n nE + eD_n \frac{dn}{dx} = j_n \tag{18}$$

In normalized form, (18) becomes

$$\frac{L_D}{V_t} n E + \frac{dn}{dx} = -\frac{J}{J_1} = -J \tag{19}$$

where

$$J_1 \equiv \frac{eD_n p_p}{L_D} \tag{20}$$

and $J \equiv -j_n$, so that $J$ represents conventional current density flowing in the $-x$ direction and is a positive quantity. The normalizing current density $J_1$ represents the diffusion current density which would be carried by an electron density falling linearly from $p_p$ to zero over a Debye length. In round numbers, $J_1 \approx 2.5 \times 10^3$ amp/cm$^2$ for 2 ohm-cm p-type germanium.

Equation (19) is a differential equation for the electron density within the transition region, and its solution consists of the sum of a complementary function (CF), and a particular integral (PI) which is a function of the current. The CF for $\underset{\sim}{n}$ is the Boltzmann factor term already given by equation (16), or by (17) after the square-law dependence of voltage upon distance is introduced. It has been seen that the density given by (17) is extremely small throughout most of the transition region, and so the PI for $\underset{\sim}{n}$ in the solution of (19) will be dominant.

The nature of the PI for $\underset{\sim}{n}$ may be determined by physical consideration of what happens to the electrons as they are injected at the plane $x = 0$. The electric field $E$ is zero at $x = 0$ and increases linearly with $x$. It follows that all the injected current is carried by diffusion at $x = 0$, but that the drift mechanism should begin to dominate as the field increases with distance into the transition region. At values of $x$

where diffusion is negligible, the second term in (19) may be dropped, and the solution for $\underset{\sim}{n}$, after substitution for $E$ from (11), is

$$\underset{\sim}{n} = \frac{\underset{\sim}{J}}{\underset{\sim}{x}} \tag{21}$$

At values of $x$ where drift is negligible (that is, close to $x = 0$), the first term in (19) may be dropped and hence

$$\frac{d\underset{\sim}{n}}{d\underset{\sim}{x}} = - \underset{\sim}{J} \tag{22}$$

There will clearly be a certain value $x = x'$ for which the drift and diffusion components of current will be equal; this value is found by differentiating (21) and setting the result equal to (22). This gives $\underset{\sim}{x}' = 1$, or $x' = L_D$. We conclude that the injected electron current is carried entirely by diffusion at $x = 0$, approximately half by diffusion and half by drift at $x'$, and primarily by drift thereafter, until the CF for $\underset{\sim}{n}$ in the solution of (19) becomes dominant. A sketch of the complete electron distribution in the transition region may therefore be constructed as in Fig. 3. The cross-over point between diffusion and drift at $x' = L_D$ is obtained by plotting equations (21) and (22) for a current $\underset{\sim}{J}/2$, since approximately half the total injected current is carried by each mechanism at $x'$.

The value of $\underset{\sim}{n}$ at $x = 0$, which is the required boundary value $\underset{\sim}{n}_c$, is found semi-graphically from Fig. 3, and equations (21) and (22)

modified for a current $\underset{\sim}{J}/2$, to be

$$\underset{\sim}{n}_c = \frac{\underset{\sim}{J}/2}{\underset{\sim}{x}'} + (\underset{\sim}{J}/2)\underset{\sim}{x}' = \underset{\sim}{J} \qquad (23)$$

since $\underset{\sim}{x}' = 1$, and hence increases linearly with injected current. This result is only approximate because the actual density gradient at $x = x'$ is less than that calculated from the drift component for $\underset{\sim}{J}/2$. The more rigorous solution of equation (19) given in section 3 leads to

$$\underset{\sim}{n}_c = 1.25\underset{\sim}{J} \qquad (24)$$

and so the above semi-quantitative argument gives a result correct within a factor of 1.25.

It is interesting to note the qualitative dependence of the transition region thickness, and of the electron density distribution within the transition region, upon the externally-imposed parameters $V_c$ and $J$. Since the injected electron density has been everywhere neglected compared to the acceptor ion density, the transition region is a depletion region, as in the conventional theory, and its thickness is a function only of the total voltage and is independent of the injected current. The electron density consists of the sum of a complementary function, which is the conventional result in the Boltzmann factor, and a particular integral, which contains drift and diffusion components dependent upon the injected current. If the reverse-bias voltage is increased, the CF

for $\underset{\sim}{n}$ continues to fall off very rapidly from $\underset{\sim}{n}_n$ very close to the metallurgical junction, but the two PI components of $\underset{\sim}{n}$ are independent of $\underset{\sim}{V}_c$ and remain fixed relative to the lower transition region boundary in Fig. 3; however, this boundary moves further downward as the transition region thickness increases with $V_c$. If the injected current increases, the transition-region thickness remains the same, and the PI components are scaled to the right in Fig. 3. Contrary to the conventional theory, therefore, in which the PI components are neglected, the actual electron density is controlled solely by the injected current throughout almost the entire transition region.

## 2.2. High-level injection in the transition region; $\underset{\sim}{n} \gg 1$

The above solution for the electron density in the transition region indicates that the boundary value $\underset{\sim}{n}_c$ increases proportionately with the injected current. For large injected currents, therefore, the value of $\underset{\sim}{n}$ within the transition region could exceed unity, that is, the injected electron density becomes greater than the equilibrium majority carrier density. Consequently the net charge density in the transition region is no longer equal to the acceptor ion density, and the electric field and potential distributions will change. We now consider the modifications in the electron density distribution necessitated by this condition.

If it is assumed that the injected current is so high that $\underset{\sim}{n} \gg 1$ everywhere in the transition region, the net charge density is dominated

by the electron charge, and the acceptor ion charge density is negligible. Conditions for space-charge-limited flow of electrons are therefore established, in which the thickness of the transition region adjusts itself to satisfy simultaneously the externally-imposed boundary values of reverse-bias voltage and injected current.

The electron density is still given by the solution of equation (19), which again consists of the sum of a complementary function and a particular integral, but the electric field now becomes current-dependent. The modified Poisson equation is

$$\frac{dE}{dx} = - \frac{e}{\epsilon}(N_A + n) \tag{25}$$

or in normalized form:

$$\frac{L_D}{V_t} \frac{dE}{d\underset{\sim}{x}} = - (1 + \underset{\sim}{n}) \tag{26}$$

It may be seen qualitatively that the electric field will be higher than in the low-injection case, since the net charge density is increased by the injected electrons; hence it may be assumed that the injected current is carried primarily by drift throughout most of the transition region, so that for the purpose of calculating $E$ we may write

$$e\mu_n nE = j_n \tag{27}$$

or in normalized form:

$$\underset{\sim}{n}\frac{L_D}{V_t}\underset{\sim}{E} = -\underset{\sim}{J} \tag{28}$$

Elimination of $\underset{\sim}{n}$ from (26) and (28), with use of the condition $\underset{\sim}{n} \gg 1$ for high-level injection, gives

$$\frac{L_D^{\,2}}{V_t^{\,2}}\underset{\sim}{E}\frac{d\underset{\sim}{E}}{d\underset{\sim}{x}} = \underset{\sim}{J} \tag{29}$$

Integration, with $E = 0$ when $x = 0$, leads to

$$\underset{\sim}{E} = -\frac{\sqrt{2}V_t}{L_D}\underset{\sim}{J}^{1/2}\,\underset{\sim}{x}^{1/2} \tag{30}$$

A second integration, with $V = 0$ at $x = 0$, gives

$$\underset{\sim}{V} = \left(\frac{2\sqrt{2}}{3}\right)\underset{\sim}{J}^{1/2}\,\underset{\sim}{x}^{3/2} \tag{31}$$

Since $V = V_c + V_i = V_{ci}$ when $x = w_t$, the transition region thickness is given by

$$\underset{\sim}{w}_t = \left(\frac{3}{2\sqrt{2}}\right)^{2/3}\frac{\underset{\sim}{V}_{ci}^{\,2/3}}{\underset{\sim}{J}^{1/3}} = 1.04\,\frac{\underset{\sim}{V}_{ci}^{\,2/3}}{\underset{\sim}{J}^{1/3}} \tag{32}$$

The transition region thickness therefore increases more rapidly with reverse bias voltage than in the low injection case, but decreases with increasing injected current.

A semi-quantitative argument analogous to that for the low injection case may now be followed. The graphical constructions are shown in Fig. 4. The Boltzmann factor contribution to the electron density, the CF for $\underset{\sim}{n}$, is still given by equation (16), but because of the three-halves power law dependence of the voltage upon distance given by equation (31), the distance dependence of the density becomes

$$\underset{\sim}{n} = \underset{\sim}{n}_n e^{-[1-(\underset{\sim}{x}/\underset{\sim}{w}_t)^{3/2}]\underset{\sim}{V}_{ci}} \tag{33}$$

where $\underset{\sim}{w}_t$ is given by equation (32). The PI for $\underset{\sim}{n}$, where this is determined only by drift current, is given by (28) with $E$ eliminated by (30):

$$\underset{\sim}{n} = \frac{1}{\sqrt{2}} \frac{\underset{\sim}{J}^{1/2}}{\underset{\sim}{x}^{1/2}} \tag{34}$$

Where the PI is determined only by diffusion current, near $x = 0$,

$$\frac{d\underset{\sim}{n}}{d\underset{\sim}{x}} = - \underset{\sim}{J} \tag{35}$$

as before. The contributions of drift and diffusion are equal at a value of $x = x'$ such that $d\underset{\sim}{n}/d\underset{\sim}{x}$ from (34) for $\underset{\sim}{J}/2$ is equal to that

given by (35) for $\underset{\sim}{J}/2$, whence

$$\underset{\sim}{x}' = \frac{1}{2^{2/3}} \frac{1}{\underset{\sim}{J}^{1/3}} = 0.63 \frac{1}{\underset{\sim}{J}^{1/3}} \tag{36}$$

The boundary value $\underset{\sim}{n}_c$ is then given by

$$\underset{\sim}{n}_c = \frac{1}{\sqrt{2}} \frac{(\underset{\sim}{J}/2)^{1/2}}{\underset{\sim}{x}'^{1/2}} + (\underset{\sim}{J}/2)\underset{\sim}{x}'$$

$$= \frac{3}{2^{5/3}} \underset{\sim}{J}^{2/3} = 0.95 \underset{\sim}{J}^{2/3} \tag{37}$$

and hence increases less than proportionately with injected current. The more rigorous solution given in section 3 leads to

$$\underset{\sim}{n}_c = 0.94 \underset{\sim}{J}^{2/3} \tag{38}$$

and so the above semi-quantitative argument gives a very accurate result.

It may be objected that there is a circularity of argument in the high-level injection case, in that the electric field distribution is calculated on the assumption that all the current flow is by drift and yet a diffusion component is subsequently accounted for in determining the boundary value of the density. This procedure may be defended on the grounds that the diffusion component is only important where the field is very small, hence little error is incurred in calculating the electric

field distribution with neglect of the diffusion component. This procedure is, in fact, commonly employed in the solution of the dielectric diode,[5] in which conditions accompanying space-charge-limited current flow are identical in principle with those discussed here. The final step of the procedure, calculation of the diffusion component near $x = 0$, could likewise be used to estimate the carrier density at the cathode of a dielectric diode.

The qualitative dependence of the transition region thickness and the electron density distribution upon the externally-imposed conditions $V_c$ and $J$ are different from the low injection level case. Since the injected electron density has been assumed everywhere large compared to the acceptor ion density, the transition region is an accumulation region, and the electric field in which the injected electrons move is modified by the presence of electron space charge. The transition region thickness therefore is a function both of the total voltage and of the injected current. The electron density again consists of the sum of a complementary function which is the conventional Boltzmann factor term, and a particular integral which is current dependent. The nature of the electron density distribution is similar to that for low-level injection, but the functional dependences on $V_c$ and $J$ are slightly different.

The salient features of the transition region properties, from an external point of view, may be summarized as follows. For small injected currents the boundary value of the injected electron density increases linearly with current at small injected currents, then increases more slowly, as the two-thirds power of the current, when the injected density

exceeds the equilibrium majority carrier density. The transition region thickness is independent of current for low injection, and becomes narrower as the one-third power of the current at high injection. The thickness increases as the one-half power of the reverse bias voltage at low injection, rising to the two-thirds power at high injection.

## 3. Case I, $v \ll v_m$: detailed quantitative treatment

In the preceding section the electron density distribution in the transition region, in the presence of injected current, was established by a semi-quantitative superposition of separate asymptotic solutions to the differential equation (19). A more detailed analytic treatment will be pursued in this section.

Since the electric field $E$ is a function of $x$, equation (19) is of a standard form and may be integrated by use of the integrating factor $\exp[(L_D/V_t)\int E\, dx] = \exp(-V)$. The result is

$$n e^{-V} = -J \int_0^x e^{-V} dx + C \tag{39}$$

where the integration constant $C$ may be determined from the boundary condition $n = n_n$, $V = V_{ci}$ when $x = w_t$, to give

$$n = n_n e^{-(V_{ci}-V)} + J e^{V} \left[ \int_0^{w_t} e^{-V} dx - \int_0^x e^{-V} dx \right] \tag{40}$$

The remaining integrations can be performed, and $\underset{\sim}{n}$ found as a function of $\underset{\sim}{x}$, if the potential $\underset{\sim}{V}$ as a function of $\underset{\sim}{x}$ is known. The previous discussion has shown that two limiting cases may be considered: first, for low-level injection, $\underset{\sim}{n} \ll 1$, the potential throughout the transition region is determined solely by the total applied voltage, and is given by equation (12); second, for high-level injection, $n \gg 1$, space-charge-limited current flow occurs and the potential is determined by both the total applied voltage and the injected current, and is given by equation (31). The expressions for the potential in both cases may be combined into a single function of the form

$$\underset{\sim}{V} = 2^{a}(8\underset{\sim}{J}/9)^{b}\ \underset{\sim}{x}^{m} \tag{41}$$

where the exponents take a different set of numerical values for each case:

| | a | b | m |
|---|---|---|---|
| $\underset{\sim}{n} \ll 1$ | -1 | 0 | 2 |
| $\underset{\sim}{n} \gg 1$ | 0 | 1/2 | 3/2 |

The advantage of introducing the general form (41) is that a single derivation, following the substitution of (41) into (40), contains both the low and high injection results as special cases.

A more elegant display is achieved if the solution of equation (40) is performed in terms of $\underset{\sim}{V}$ rather than of $\underset{\sim}{x}$. The result is

$$\underset{\sim}{n} = \underset{\sim}{n}_n e^{-(\underset{\sim}{V}_{ci}-\underset{\sim}{V})} + \frac{(9/8)^{b/m}}{2^{a/m}}\left(\frac{1}{m!}\right)\underset{\sim}{J}^{1-b/m}\, e^{\underset{\sim}{V}}\left[E_m(\underset{\sim}{V}_{ci}^{1/m}) - E_m(\underset{\sim}{V}^{1/m})\right] \tag{42}$$

where

$$\left(\frac{1}{m!}\right)E_m(u) \equiv \int_0^u e^{-u^m}\,du$$

is a tabulated integral.[6] Equation (42), together with (41), defines the electron density distribution as a function of distance through the transition region. The boundary value $\underset{\sim}{n}_c$ at $\underset{\sim}{x} = 0$ is found by putting $\underset{\sim}{V} = 0$ in (42):

$$\underset{\sim}{n}_c = \underset{\sim}{n}_n e^{-\underset{\sim}{V}_{ci}} + \frac{(9/8)^{b/m}}{2^{a/m}}\left(\frac{1}{m!}\right)\underset{\sim}{J}^{1-b/m}\, E_m(\underset{\sim}{V}_{ci}^{1/m}) \tag{43}$$

Since $\underset{\sim}{V}_{ci} = \underset{\sim}{V}_c + \underset{\sim}{V}_i$ and $\underset{\sim}{n}_n \exp(-\underset{\sim}{V}_i) = \underset{\sim}{n}_p$, and since the function $E_m(\underset{\sim}{V}_{ci}^{1/m})$ is very close to unity even for $V_c = 0$ (because $\underset{\sim}{V}_i = V_i/V_t \gg 1$), equation (43) may be rewritten

$$\underset{\sim}{n}_c = \underset{\sim}{n}_p e^{-\underset{\sim}{V}_c} + \frac{(9/8)^{b/m}}{2^{a/m}}\left(\frac{1}{m!}\right)\underset{\sim}{J}^{1-b/m} \tag{44}$$

This result verifies the presence of a current-dependent term in addition to the familiar Boltzmann factor term. For reverse biases and non-zero injected currents of practical interest, the Boltzmann factor term is entirely negligible.

For completeness, the two special cases of equation (44) may be obtained by substitution of the appropriate values of the exponents a, b, and m. For low-level injection, $\underset{\sim}{n} \ll 1$,

$$\underset{\sim}{n}_c = \sqrt{\frac{\pi}{2}}\, \underset{\sim}{J} = 1.25\, \underset{\sim}{J} \tag{45}$$

and for high-level injection, $\underset{\sim}{n} \gg 1$,

$$\underset{\sim}{n}_c = \left(\frac{9}{8}\right)^{1/3}\left(\frac{21}{3}\right)\underset{\sim}{J}^{2/3} = 0.94\, \underset{\sim}{J}^{2/3} \tag{46}$$

where the Boltzmann factor term is neglected in both cases.

Equations (45) and (46) are the results of greatest interest from the point of view of overall transistor performance. However, the nature of the electron density distribution in the transition region is of interest in its own right. Equation (42) may be rearranged to eliminate $\underset{\sim}{J}$ in favor of $\underset{\sim}{n}_c$, by equation (43), to give

$$\underset{\sim}{n} = \left[\frac{E_m(\underset{\sim}{V}^{1/m})}{E_m(\underset{\sim}{V}_{ci}^{\,1/m})}\right] \underset{\sim}{n}_n e^{-(\underset{\sim}{V}_{ci}-\underset{\sim}{V})} + \left[1 - \frac{E_m(\underset{\sim}{V}^{1/m})}{E_m(\underset{\sim}{V}_{ci}^{\,1/m})}\right] \underset{\sim}{n}_c e^{\underset{\sim}{V}} \tag{47}$$

Interpretation of the form (47) shows that $\underset{\sim}{n}$ is dominated by the term in $\underset{\sim}{n}_c$ from $\underset{\sim}{V} = 0$ (the edge of the neutral p-region) until $\underset{\sim}{V}$ becomes very nearly equal to $\underset{\sim}{V}_{ci}$ (just before the metallurgical junction). Throughout most of the transition region, where $\underset{\sim}{n}$ is dominated by the term in $\underset{\sim}{n}_c$, two asymptotic forms of (47) may be obtained, depending upon whether $\underset{\sim}{V}^{1/m}$ is much less than or much greater than unity. For both low and high injection conditions, $\underset{\sim}{V}^{1/m} \ll 1$ corresponds to $\underset{\sim}{x} \ll \underset{\sim}{x}'$, as may be seen by substituting the appropriate expression for $\underset{\sim}{x}'$ and the values of the exponents in equation (41). Thus $\underset{\sim}{V}^{1/m} \ll 1$ corresponds to the region close to the injection plane where diffusion is dominant, and series expansion of (47) for this condition gives

$$\underset{\sim}{n} \approx \underset{\sim}{n}_c \left( 1 - \frac{\underset{\sim}{V}^{1/m}}{(1/m)!} \right) (1 + \underset{\sim}{V}) \tag{48}$$

Differentiation of (48) with respect to $\underset{\sim}{x}$ and substitution for $\underset{\sim}{n}_c$ and $\underset{\sim}{V}$ verifies that $d\underset{\sim}{n}/d\underset{\sim}{x} = -\underset{\sim}{J}$ at $\underset{\sim}{x} = 0$ for either low or high injection level, thus at injection all the current is carried by diffusion. The condition $\underset{\sim}{V}^{1/m} \gg 1$ corresponds to $\underset{\sim}{x} \gg \underset{\sim}{x}'$ where drift is dominant, and appropriate expansion of equation (47) leads to

$$\underset{\sim}{n} \approx \underset{\sim}{n}_c \frac{1}{(1/m)!} \frac{\underset{\sim}{V}^{-(1-1/m)}}{mE_m(\underset{\sim}{V}_{ci}^{1/m})} \left[ 1 - \left( \frac{\underset{\sim}{V}}{\underset{\sim}{V}_{ci}} \right)^{1-1/m} e^{\underset{\sim}{V}-\underset{\sim}{V}_{ci}} \right] \tag{49}$$

Substitution for $\underset{\sim}{n}_c$ and $\underset{\sim}{V}$ gives the distribution explicitly as a function of distance with the injected current as parameter:

$$\underset{\sim}{n} \approx \frac{9}{8}\frac{(8\underset{\sim}{J}/9)^{1-b}}{m2^a\ \underset{\sim}{x}^{m-1}}\left[1 - \left(\frac{\underset{\sim}{x}}{\underset{\sim}{w}_t}\right)^{m-1} e^{-\underset{\sim}{V}_{ci}[1-(\underset{\sim}{x}/\underset{\sim}{w}_t)^m]}\right] \qquad (50)$$

The term in the square brackets in equations (49) and (50) is essentially equal to unity until $\underset{\sim}{V}$ is very nearly equal to $\underset{\sim}{V}_{ci}$, or $\underset{\sim}{x}$ is very close to $\underset{\sim}{w}_t$. Usually the Boltzmann factor term in (47) will dominate before this condition is reached. Throughout most of the transition region, then, for $\underset{\sim}{V}^{1/m} \gg 1$, equation (50) reduces to $\underset{\sim}{n} \approx \underset{\sim}{J}/\underset{\sim}{x}$ for low injection level, and to $\underset{\sim}{n} \approx (1/\sqrt{2})\ \underset{\sim}{J}^{1/2}/\underset{\sim}{x}^{1/2}$ for high injection level, in accordance with the previous semi-quantitative discussion.

Figures 5 through 7 show the injected electron density as a function of distance through the transition region under three conditions, plotted from equation (47) with use of (41). The external collector voltage $V_c$ is set at 1 v throughout, and the internal contact potential $V_i$ is taken to be 0.3 v, so that $\underset{\sim}{V}_{ci} = 52$ for $V_t = 25$ mv. The low value of external collector voltage is chosen so that the Boltzmann factor term is visible on the same distance scale that is appropriate for the second term in (47). The equilibrium majority carrier density in the collector n-region is taken to be 100 times that in the p-region, so that $\underset{\sim}{n}_n = 100$. Figure 5 shows the electron distribution for the low injection level condition $\underset{\sim}{J} = 10^{-2}$, when the normalized transition region thickness is given by equation (15) as $\underset{\sim}{w}_t = 10.2$. Figure 6 is for the high injection condition $\underset{\sim}{J} = 10^{2}$, when the normalized transition region

thickness is given by equation (32) as $\underset{\sim}{w}_t = 3.2$. In both Figs. 5 and 6, the asymptotes and approximate boundary value $\underset{\sim}{n}_c$ as described in the semi-quantitative treatment are given for comparison. Results illustrating the decrease in density, before the final increase due to the Boltzmann factor term, have been obtained independently by Sparkes,[7] who used a numerical integration method. Figure 7 is for the even higher injection condition $\underset{\sim}{J} = 10^5$, chosen to illustrate a rapid fall rather than a rapid rise in density just in front of the metallurgical junction. This occurs because the term in the square brackets in equation (50) drops significantly below unity before the Boltzmann factor contribution to the density begins to dominate. The normalized transition region thickness for $\underset{\sim}{J} = 10^5$, again given by equation (32), is $\underset{\sim}{w}_t = 0.32$. Only the part of the transition region close to the metallurgical junction is shown in Fig. 7, since the remaining part is the same as in Fig. 6 with the density scale multiplied by $1000^{2/3} = 100$, and the distance scale divided by $1000^{1/3} = 10$.

A composite picture of the electron distribution for the three injection currents $\underset{\sim}{J} = 10^{-2}$, $10^2$, and $10^5$, is shown in Fig. 8 for the three external collector voltages $V_c = 1$ v, 10 v, and 20 v. The dependence of the boundary value $\underset{\sim}{n}_c$ upon the injected current $\underset{\sim}{J}$ is also shown. Equation (15) or (32), as appropriate, is used to determine the transition region thickness. A logarithmic density scale is used to accommodate the range of injection levels. For $\underset{\sim}{J} = 10^5$, the distribution only for $V_c = 20$ v is shown to prevent crowding of the picture. This figure illustrates the joint dependence of the transition region

thickness upon both the applied voltage and the injected current.

4. Case II, $v = v_m$

The discussion of the preceding sections has been based on the assumption that the injected electron velocity in the transition region is everywhere less than the limiting value $v_m$, so that the usual equations of drift and diffusion flow could be employed. We may examine the validity of this assumption by calculating the electron velocity required by the solutions obtained.

For low-level injection, the electric field in the transition region is linear in distance and is given by equation (7). The electron velocity is $v = -\mu_n E$ when most of the current is carried by drift, as occurs throughout most of the transition region approximately between $x = L_D$ and $x = w_t$. For a 1-v external reverse bias, $w_t \approx 10L_D$, hence $v(L_D) = -\mu_n E(L_D) = \mu_n V_t/L_D = D_n/L_D$, and $v(w_t) = 10D_n/L_D$. In round numbers, $D_n = 93$ cm$^2$/v-sec and $L_D = 10^{-5}$ cm for 2 ohm-cm p-type germanium, hence $v(L_D) \approx 10^7$ cm/sec and $v(w_t) \approx 10^8$ cm/sec. The limiting electron drift velocity is not far below this order of magnitude range,[8] and so it may be concluded that the basic assumption is not valid for the conductivity chosen. If the p-region conductivity approaches the intrinsic value, the Debye length increases by about an order of magnitude, and so the required electron velocity decreases by the same factor. Thus for low conductivity material, such as would occur in an epitaxial layer under the collector region, it may be reasonable to assume that the usual equations of drift and diffusion current

apply and the analysis of the preceding sections is applicable. The accuracy of this assumption is, however, only marginal, and collector reverse biases higher than a volt will increase the required electron velocity even closer to the limiting value.

For alloy transistors, in which the base resistivity is in the order of 2 ohm-cm, and for diffused-base transistors, in which the built-in field causes the carrier drift velocity to approach its limiting value, the basic assumption of the preceding sections is untenable. It is therefore reasonable to make the opposite assumption, namely that the injected electrons travel with an essentially constant velocity equal to the maximum drift velocity $v_m$ throughout most of the transition region. In this case the injected current density may be written

$$J = env_m \tag{51}$$

and the normalized electron density $\underset{\sim}{n}$ is therefore given by $\underset{\sim}{n} = J/J_2$, where

$$J_2 \equiv ep_p v_m \tag{52}$$

is the current density which would be carried by an electron density equal to the equilibrium majority carrier density moving with the limiting drift velocity. In round numbers, $J_2 \approx 1.8 \times 10^3$ amp/cm$^2$ for 1 ohm-cm p-type germanium if $v_m$ is taken as $6 \times 10^6$ cm/sec. Finally, we may

write

$$\underset{\sim}{n} = \underset{\sim}{J} \tag{53}$$

where now the bold-face $\underset{\sim}{J}$ indicates normalization with respect to $J_2$ instead of $J_1$.

In Case II, equation (53) replaces the asymptotic drift current form of equation (21) for Case I, and is applicable throughout most of the transition region. Very close to the metallurgical junction, nevertheless, the electron density must again undergo a rapid change to meet the boundary value $\underset{\sim}{n}_n$, and very close to the neutral p-region diffusion must again become dominant since the field goes to zero. However, we have seen in the previous discussion, and from Figs. 3 and 4, that the diffusion component near $x = 0$ gives rise to only a small change in the boundary value $\underset{\sim}{n}_c$ from the value of $\underset{\sim}{n}$ which exists when the drift component takes over; there is therefore little error incurred in applying equation (53) at $x = 0$, so that the boundary value of the injected electron density is obtained directly as

$$\underset{\sim}{n}_c = \underset{\sim}{J} \tag{54}$$

The result $\underset{\sim}{n}_c = \underset{\sim}{J}$ is applicable to both low and high injection levels, thus the increase in the boundary value is linear with injected current under all conditions, and does not give way to a two-thirds

power law at high injection. It is shown in the companion paper [4] that the modified collector boundary value introduces little departure of the overall transistor performance parameters from the results obtained with the conventional zero boundary value, hence some inaccuracy in the numerical factor in equation (54) is of little ultimate significance.

In Case II, the transition region is again a depletion region at low-level injection, and so its thickness and voltage-dependence are the same as in Case I, given by equation (15). At high-level injection, the transition region becomes an accumulation region but the constant electron density distribution with distance in Case II, given by equation (53), leads to voltage and current dependences of the transition region thickness which are different from those in Case I. An expression for $w_t$ may be obtained by substituting equation (53) directly into Poisson's equation (25):

$$\frac{L_D}{V_t} \frac{dE}{dx} = - (1 + J) \tag{55}$$

Since $J$ is independent of $x$, $E$ is linear in $x$, as at low injection level, and the result for $w_t$ is

$$w_t = \sqrt{2} \frac{V_{ci}^{1/2}}{(1 + J)^{1/2}} \tag{56}$$

The transition region therefore again decreases with increasing current at high injection levels, and at a faster rate than in Case I. The

voltage dependence, however, remains the same as at low-level injection, and does not give way to a two-thirds power law as occurs in Case I.

A composite picture of the injected electron distribution for Case II is shown in Fig. 9, for the same three currents and voltages employed in Fig. 8 for Case I. The departure from equation (53) near $\underset{\sim}{x} = 0$ is neglected, and the rapid change near $\underset{\sim}{x} = \underset{\sim}{w}_t$ is not calculated exactly since the change occurs over such a small distance. For the purpose of transistor analysis, the boundary value $\underset{\sim}{n}_c$ given by (54) and the transition region thickness $\underset{\sim}{w}_t$ given by (56) are the most important results.

## 5. Conclusions

It has been shown that the presence of minority carrier electron current, injected into the transition region of a reverse-biased p-n junction from the neutral p-region, has a significant effect upon the electron density distribution and the transition region thickness. Contrary to the result of the conventional solution, in which the presence of current is neglected, the electron density is determined essentially entirely by the injected current throughout most of the transition region.

In Case I, where the electron velocity is less than the limiting velocity, and description in terms of drift and diffusion currents is applicable, the electron density decreases markedly with distance from its value at injection, until the conventional Boltzmann factor contribution dominates just in front of the metallurgical junction. For

low-level injection, the transition region is essentially completely depleted of mobile carriers and the injected electrons move in an electric field which is determined uniquely by the applied voltage. The electron density at injection, the boundary value $n_c$, increases proportionately with the injected current, and the transition region thickness $w_t$ increases as the square root of the total junction voltage but is independent of the current. For high-level injection, electron accumulation occurs in the transition region, and conditions of space-charge-limited flow are established in which the injected electrons move in a field which is a function both of the applied voltage and of the current. The boundary value of the electron density then increases as the two-thirds power of the injected current, more slowly than at low injection level. The transition region thickness increases as the two-thirds power of the total voltage, faster than at low-level injection, but decreases as the one-third power of the injected current. The results of Case I are applicable to junctions in which the conductivity of the p-region is low, as would occur in an epitaxial layer under the collector of an n-p-n transistor.

In Case II, where the electron velocity is equal to the limiting velocity, the electron density remains essentially constant with distance at its injection value $n_c$, until the conventional Boltzmann factor dominates. The boundary value $n_c$ is directly proportional to the current regardless of injection level, and therefore increases more rapidly at high-level injection than in Case I. At low-level injection, the transition region thickness is again independent of current and

increases as the square root of the total voltage, but at high-level injection carrier accumulation occurs and current dependence appears. Since the electron distribution remains uniform at high-level injection, the transition region thickness continues to increase as the square root of the total voltage, but decreases as the square root of the current when the electron space charge dominates over the fixed acceptor ion charge. The results of Case II are applicable to junctions in which the conductivity of the p-region is fairly high, as in alloy transistors, or in which a built-in field accelerates the mobile carriers to limiting velocity even at low currents, as in diffused-base transistors.

When a reverse-biased p-n junction is used as the collector junction of an n-p-n transistor, the quantities of primary interest, from the point of view of the overall transistor performance, are the thickness of the transition region and the boundary value of the minority carrier density at the edge of the transition region. Conventional p-n junction theory states that, under conditions of reverse bias, the transition region thickness is a function only of the voltage, and the boundary value of the density is essentially zero. It has been shown, however, that in the presence of minority carrier current injected from the emitter, the boundary value of the density increases with the current and the transition region thickness becomes smaller at high currents. These modified boundary conditions should therefore be taken into account in the basic analysis of transistor operation.

Acknowledgements

Valuable discussions with and suggestions by J. J. Sparkes and M-A. Nicolet are gratefully acknowledged. The work was supported in part by funds made available by the Jet Propulsion Laboratory of the California Institute of Technology from NASA Contract No. NAS 7-100.

## References


1. W. Shockley, Bell Syst. Tech. J., 28, 435, (1949).

2. A. W. Matz, J. Electronics and Control, 7, 133, (1959).

3. C. T. Kirk, I.R.E. Trans. on Electron Devices, ED-9, 164, (1962).

4. R. D. Middlebrook, Solid State Electronics,

5. W. Shockley and R. C. Prim, Phys. Rev., 90, 753, (1953).

6. E. Jahnke and F. Emde, Tables of Functions, Dover, New York.

7. J. J. Sparkes, personal communication.

8. A. F. Gibson and J. W. Granville, J. Electronics and Control, 2, 259, (1956).

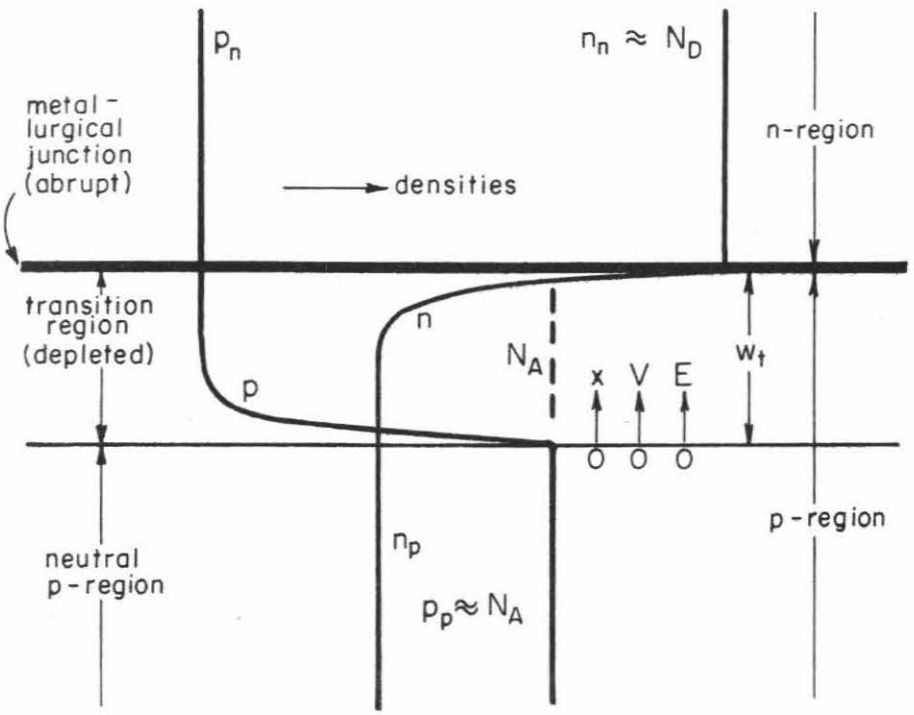


Fig. 1. Model of a p-n junction in thermal equilibrium. The conductivity of the n-region is taken to be much greater than that of the p-region, so that the transition region lies essentially entirely within the p-region.

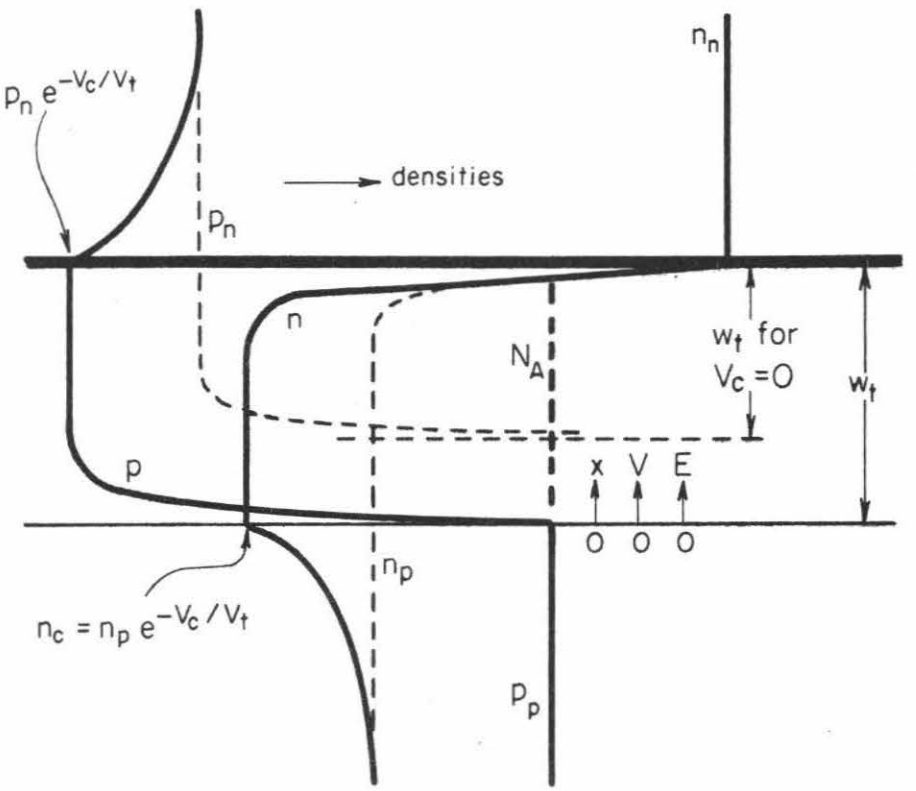


Fig. 2. Conditions in the p-n junction of Fig. 1 when reverse-biased by a voltage $V_c$ (n-region positive), for zero injected current from the p-region (conventional solution). The boundary value $n_c$ is essentially zero.

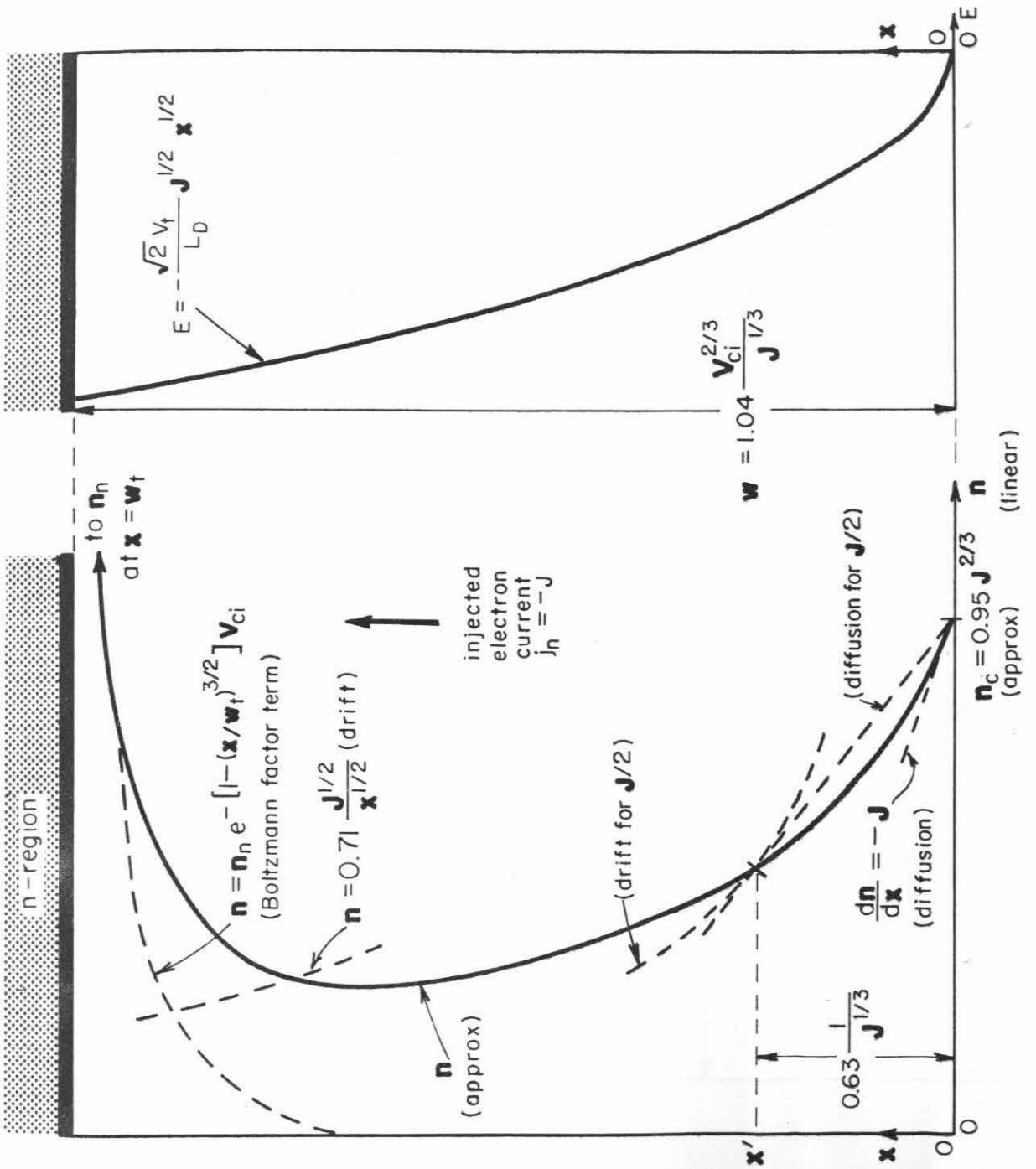


Fig. 3. Semi-quantitative solution for the electron density in the transition region of a p-n junction under conditions of external reverse bias $V_c$ and injected electron current J. Valid for low injection level, $\underline{n} \ll 1$. (Not drawn to scale.)

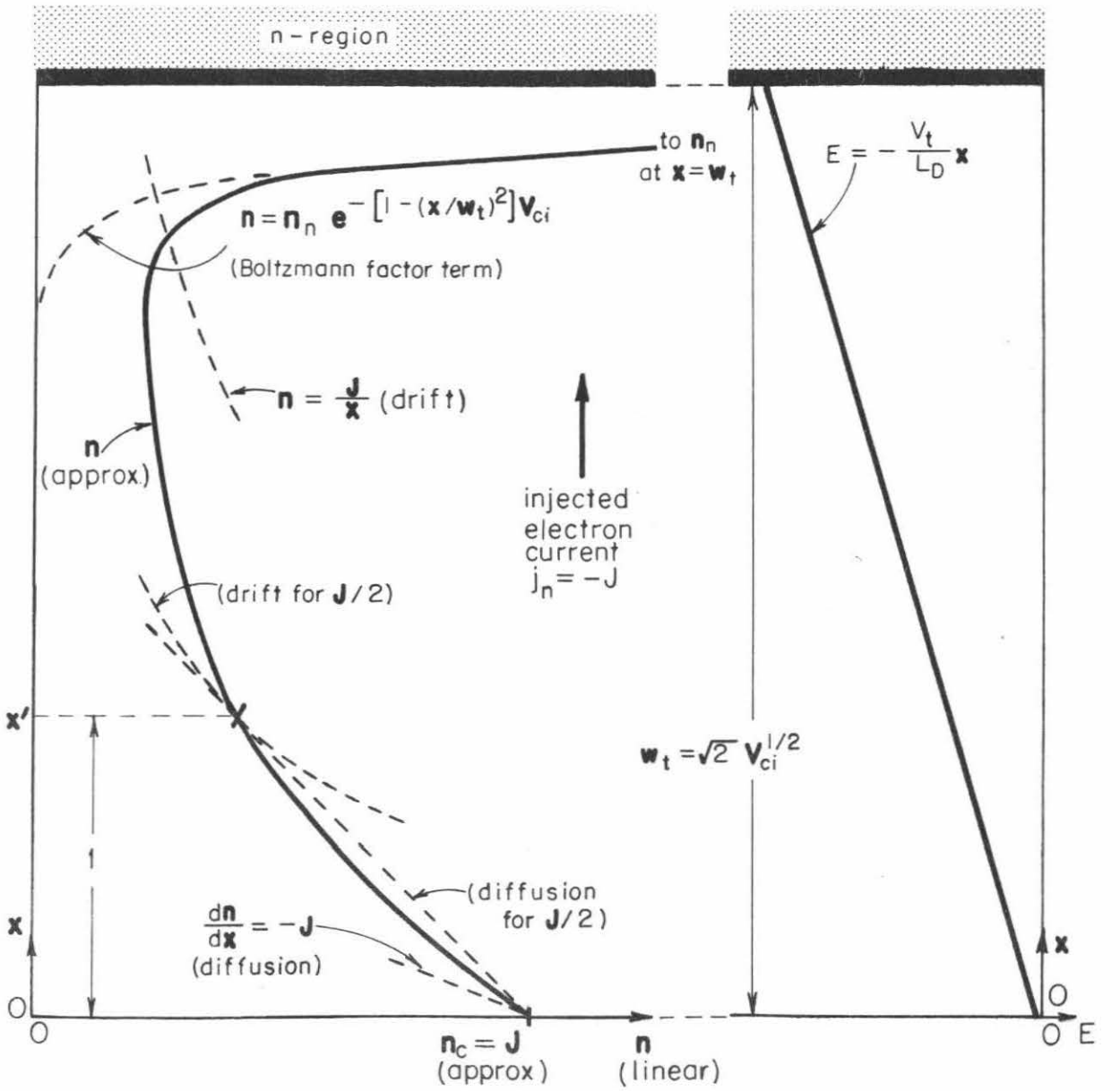


Fig. 4. As Fig. 3, but for high injection level, $n \gg 1$. (Not drawn to scale.)

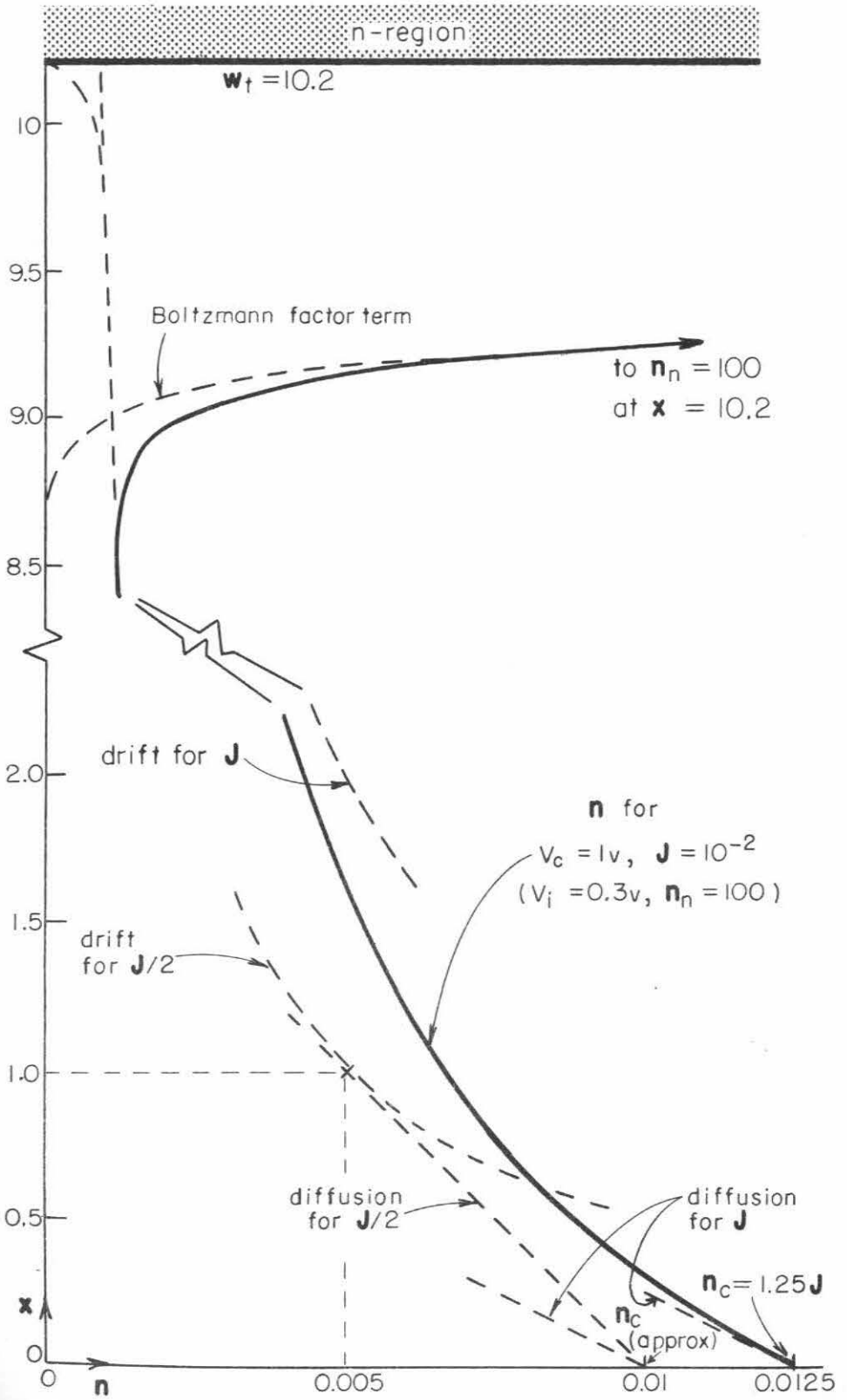


Fig. 5. Electron density plotted from equation (47), for the low injection level case $J = 10^{-2}$.

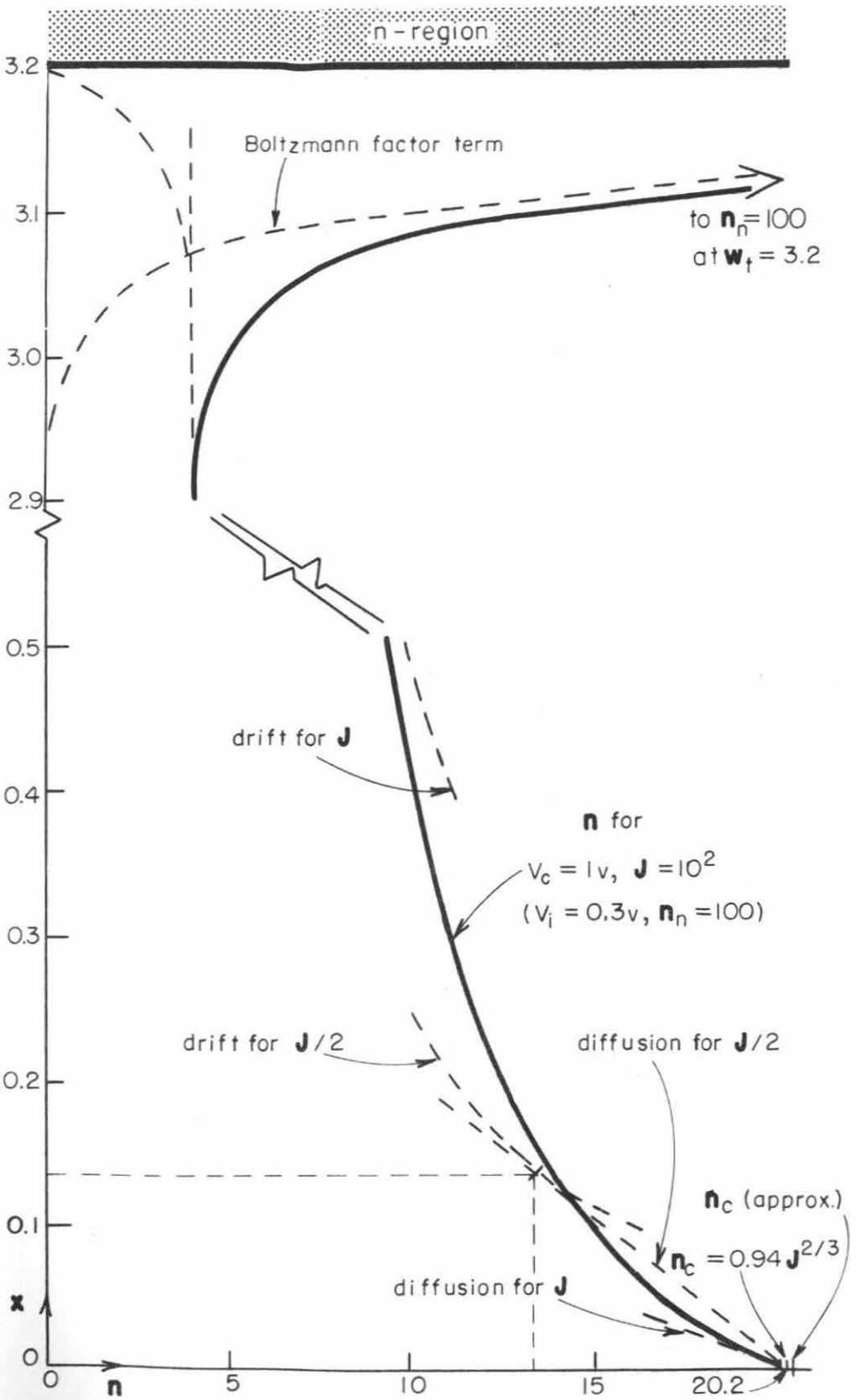


Fig. 6. Electron density plotted from equation (47), for the high injection level case $J = 10^2$.

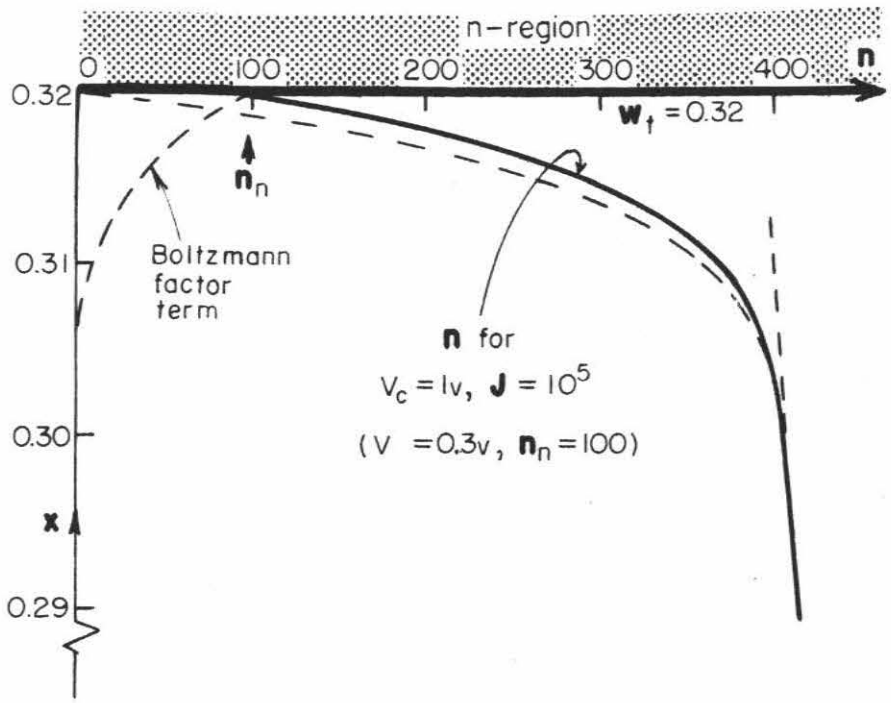


Fig. 7. Electron density close to the metallurgical junction, plotted from equation (47), for the high injection level case $J = 10^5$.

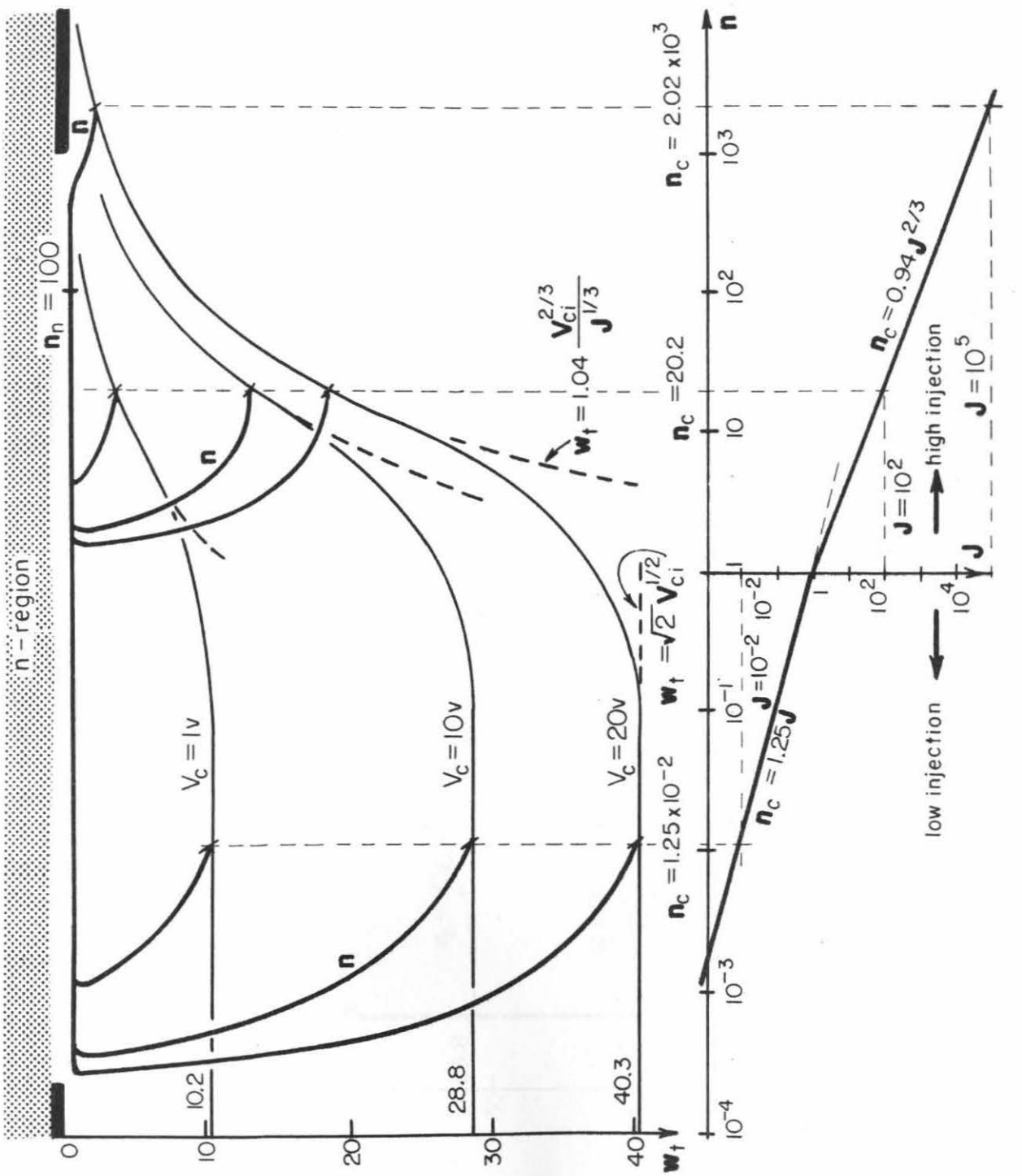


Fig. 8. Plots of electron density distribution $\underset{\sim}{n}$ and transition region thickness $\underset{\sim}{w_t}$ for Case I, $v \ll v_m$. A subsidiary graph shows the dependence of the boundary value $\underset{\sim}{n_c}$ upon the injected current $\underset{\sim}{J}$.

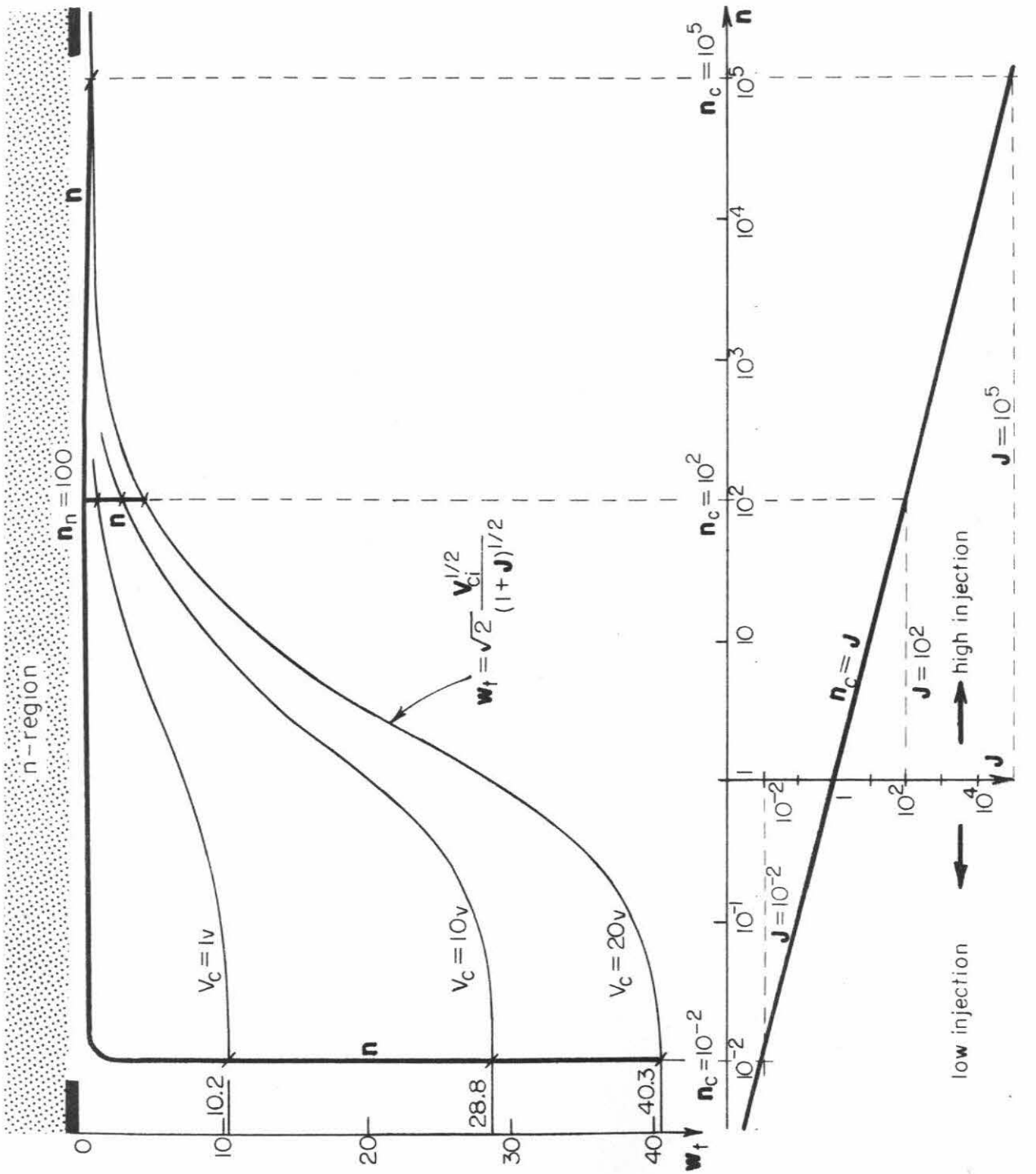


Fig. 9. As Fig. 8, but for Case II, $v = v_m$.

# EFFECTS OF MODIFIED COLLECTOR BOUNDARY CONDITIONS ON THE BASIC PROPERTIES OF A TRANSISTOR

R. D. Middlebrook

Department of Engineering and Applied Science

California Institute of Technology

Pasadena, California

Abstract

Effects due to modified collector boundary conditions in an n-p-n alloy-junction transistor are investigated. The modified boundary conditions differ from those conventionally employed in that the minority carrier density $n_c$ at the base side of the collector transition region increases with collector current $J$, and the transition region thickness $w_t$ decreases with increasing collector current when high-level injection into the collector transition region occurs. One of the two major objections to the conventional assumptions, namely that zero carrier density at the collector junction would require infinite carrier velocity, is thereby removed.

The particular performance properties examined are the collector current $J$ versus base-emitter voltage $V$ transfer characteristic, and the d-c current gain $\beta$ versus collector current $J$ characteristic. Derivation of these two characteristics is first reviewed for the conventional collector boundary conditions, partly as a tutorial exposition of the charge-control method of analysis, and partly as a foundation for the following derivations with the modified collector boundary conditions. It is shown that the second major objection to the conventional assumptions, namely that charge neutrality would not be maintained in the "neutral" base region at high-level injection, is eliminated in the modified solution.

The modified solution predicts that the $J$ versus $V$ and the $\beta$ versus $J$ characteristics differ from the conventional results by only small degrees which, in a practical transistor, will certainly be masked by many effects not represented in the simple model considered.

It is concluded, therefore, that the conventional analysis and results do in fact predict with good accuracy the performance of a transistor, within the limitations of the model, and that the major benefit of the modified collector boundary conditions is to remove two untenable assumptions and restore confidence in the conventional analysis.

Contents

# Notation

(Symbols not explicitly defined in the text)

| | |
|---|---|
| $e$ | magnitude of the electronic charge |
| $k$ | Boltzmann's constant |
| $T$ | absolute temperature |
| $\epsilon$ | permittivity |
| $n_n, n_p$ | thermal-equilibrium electron density in the neutral n-region, p-region |
| $p_n, p_p$ | thermal-equilibrium hole density in the neutral n-region, p-region |
| $D_n, D_p$ | electron, hole diffusion constant |
| $\mu_n, \mu_p$ | electron, hole mobility |

## 1. Introduction

In the elementary analytical treatment of a junction transistor, the basic device properties are determined from the solution of a differential equation which describes the flow of injected minority carriers in the base region.[1] Numerous approximations are usually employed, of which one of the most important is that the physical base region is assumed to consist of a charge-neutral region separated from the metallurgical emitter and collector junctions by sharply-defined transition regions in which complete charge depletion exists. The differential equation for injected minority carrier flow is solved for the neutral base region, for a given geometry, and subject to certain boundary conditions at the edges of the neutral region.

According to conventional analysis, the required boundary values at the transition-region edges of the neutral base region are related to the emitter and collector applied voltages by simple Boltzmann factors. For an n-p-n transistor biased in the normal active operating region, the boundary value of the minority carrier electron density at the emitter edge of the neutral base region is greater than the thermal equilibrium value, but the boundary value at the collector edge is very much less than the thermal equilibrium value, and is essentially zero for collector reverse biases of more than a few tenths of a volt.

The use of a zero boundary value for the minority carrier density at the collector junction of a normally-biased transistor, almost universally accepted, is open to serious objection on two counts.[2] First, the presence of non-zero collected current would require infinite charge velocity if the density were zero, but since there is a limiting

drift velocity for mobile carriers in a solid this condition clearly cannot exist. Second, the initial assumption of charge-neutrality in the "neutral" base region is violated at high-level injection.

It is shown in a companion paper[3] that reconsideration of the collector transition region leads to modified collector boundary conditions in the presence of injected minority carrier current. The minority carrier density at the edge of the base neutral region increases with current, thus eliminating the requirement for infinite carrier velocity, and the transition region thickness, though constant for low currents, decreases at high currents.

The purpose of this paper is to investigate the effects of these modified collector boundary conditions on some of the basic terminal characteristics of a transistor. Two sets are considered: first, the collector current as a function of base-emitter voltage (common-emitter d-c transfer characteristic); second, the d-c current-gain as a function of collector current (common-emitter d-c $\beta$ versus operating current). The effects of modified collector boundary conditions upon the high-frequency cutoff are not considered here, since they have been investigated by Kirk.[4]

A summary of the conventional first-order theory of a transistor is given in section 2, and provides at once a concise review of the charge-control approach to analysis and a foundation upon which to build the effects due to the modified collector boundary conditions introduced in section 3. In section 4 a detailed treatment is given of the corrections required in the basic analysis when the modified collector boundary conditions are recognized. In section 5 it is shown that when the

modified collector boundary conditions are taken into account, the initial assumption of charge neutrality is not significantly violated, and a satisfactory disposition of both the major objections to the conventional theory is thus achieved.

## 2. Basic solution with conventional collector boundary conditions

In this section a summary is presented of the basic solution of a junction transistor when the conventional collector boundary conditions are employed. The charge control approach[5],[6] is used, in which the first-order relationships are derived with neglect of recombination, and the second-order relationships are derived by considering the perturbation due to the finite lifetime of injected carriers.

The discussion is based on the model of an n-p-n alloy junction transistor shown in Fig. 1, and incorporates the following features and assumptions. A base p-region of moderate, uniform acceptor doping density $N_A$ forms abrupt metallurgical junctions with emitter and collector n-regions of very high, uniform donor doping density $N_D$. Plane, parallel junctions are assumed and only one-dimensional current flow is considered. Because of the large ratio $N_D/N_A$, the transition regions appear almost entirely within the p-region. The transition region thicknesses are functions of the corresponding junction voltages. Since normal bias alone is to be considered (forward-biased emitter, reverse-biased collector), the emitter transition region is very thin and will be taken to be of constant width. In Fig. 1, the vertical axis is linear distance increasing upwards. The origin for distance $x$,

potential V, and electric field E is taken at the upper edge of the emitter transition region. The charge-neutral p-region is defined by $0 < x < w_{no}$, and the collector transition region is defined by $w_{no} < x < w$. The distance $w \equiv (w_{no}+w_{to})$ is essentially equal to the metallurgical base width, since the emitter transition region thickness is neglected, and is therefore a constant parameter of the device. Figure 1 also shows the qualitative distributions of carrier densities for normal bias, in which the conventional assumption is made that the electron density at each edge of the neutral p-region is related to the corresponding junction voltage by a Boltzmann factor. The horizontal density scale is distorted in order to accommodate orders of magnitude density differences while retaining the similar distribution shapes of the electron and hole densities n and p required by the neutrality condition.

The transfer characteristic, collector current J as a function of base-emitter voltage V, is a first-order property of the device and will be derived by neglecting recombination. A non-linear first-order differential equation, which has a simple analytic solution, is established for the minority carrier density in the neutral base region. Insertion of the boundary conditions in terms of the base-emitter voltage gives a complete solution for the injected minority carrier density distribution, and also the required transfer characteristic. The common-emitter d-c current gain $\beta$ is a second-order parameter, since it is directly related to recombination of injected carriers. The base current as a function of the collector current, and hence the current gain, is

found by dividing the total injected minority carrier charge in the base by the effective lifetime. The above approach, based on that of Webster[7] and extended by Middlebrook[8] and others,[9],[10] derives the transistor characteristics directly in the common-emitter configuration and avoids the undesirable and unrealistic method of first deriving the common-base characteristics.

## 2.1. The conventional J versus V transfer characteristic

The basic equations for solution of the minority carrier density $n$ in the neutral base region $0 < x < w_{no}$ are

$$-e\mu_n n\frac{dV}{dx} + eD_n \frac{dn}{dx} = j_n \tag{1}$$

$$-e\mu_p p\frac{dV}{dx} - eD_p \frac{dp}{dx} = j_p = 0 \tag{2}$$

$$p - n = p_p - n_p \approx p_p \tag{3}$$

in which equation (1) expresses the electron current density $j_n$ as the sum of drift and diffusion components, the hole current density $j_p$ in equation (2) is zero because of neglect of recombination and the assumption of very high emitter and collector conductivities, and equation (3) describes the charge neutrality condition. The emitter and

collector boundary values $n_e$ and $n_c$ of the electron density are given, conventionally, by Boltzmann factors:

$$n_e = n_p e^{V_j/V_t} \tag{4}$$

$$n_c = n_p e^{-V_c/V_t} \approx 0 \tag{5}$$

where $V_t \equiv kT/e$, $V_c$ is the collector reverse-bias voltage, and $V_j$ is the forward-bias voltage across the emitter-base transition region. The total (external) base-emitter voltage exceeds $V_j$ by an additional component $V_p$ due to the non-uniform hole density $p$. Direct integration of equation (2) shows $V_p$ to be related to the hole density $p_e$ at the emitter boundary by $p_e = p_p \exp(V_p/V_t)$, since the hole density at the ohmic base contact is equal to $p_p$. Use of the charge neutrality condition of equation (3) leads to

$$1 + \frac{n_e}{p_p} = e^{V_p/V_t} \tag{6}$$

The total (external) base-emitter forward-bias voltage $V$ is then

$$V = V_j + V_p \tag{7}$$

It is convenient to normalize the above equations before proceeding to their solution. The normalizing parameters are: density $p_p$, distance $w_{no}$, and voltage $V_t$. In order that the familiar symbols may be retained, normalized quantities will be distinguished from the originals by bold-face type, so that $\underset{\sim}{n} \equiv n/p_p$, $\underset{\sim}{x} \equiv x/w_{no}$, $\underset{\sim}{V} \equiv V/V_t$, etc. In normalized form, equations (1) through (7) read

$$\underset{\sim}{n}\frac{d\underset{\sim}{V}}{d\underset{\sim}{x}} - \frac{d\underset{\sim}{n}}{d\underset{\sim}{x}} = \frac{J}{J_0} = \underset{\sim}{J} \tag{8}$$

$$\underset{\sim}{p}\frac{d\underset{\sim}{V}}{d\underset{\sim}{x}} + \frac{d\underset{\sim}{p}}{d\underset{\sim}{x}} = 0 \tag{9}$$

$$\underset{\sim}{p} - \underset{\sim}{n} = 1 - \underset{\sim}{n}_p \approx 1 \tag{10}$$

$$\underset{\sim}{n}_e = \underset{\sim}{n}_p e^{\underset{\sim}{V}_j} \tag{11}$$

$$\underset{\sim}{n}_c = \underset{\sim}{n}_p e^{-\underset{\sim}{V}_c} \approx 0 \tag{12}$$

$$1 + \underset{\sim}{n}_e = e^{\underset{\sim}{V}_p} \tag{13}$$

$$\underset{\sim}{V} = \underset{\sim}{V}_j + \underset{\sim}{V}_p \tag{14}$$

In equation (8),

$$J_0 \equiv \frac{eD_n p_p}{w_{no}} \tag{15}$$

and $J \equiv -j_n$, so that $J$ represents conventional current density flowing in the $-x$ direction, and is the collector current density. The normalizing current density $J_0$ represents the diffusion current density which would be carried by an electron density falling linearly from $p_p$ to zero over the length of the neutral base region.

The first-order solution begins with the elimination of $d\tilde{V}/d\tilde{x}$ and $\tilde{p}$ from equations (8) and (9) by use of (10). The result is the basic differential equation for the injected minority carrier density $\tilde{n}$:

$$\frac{1 + 2\tilde{n}}{1 + \tilde{n}} \frac{d\tilde{n}}{d\tilde{x}} = -\tilde{J} \tag{16}$$

The solution is

$$2\tilde{n} - \ln(1 + \tilde{n}) = \tilde{J}(1 - \tilde{x}) + 2\tilde{n}_c - \ln(1 + \tilde{n}_c) \tag{17}$$

which shows that $\tilde{n}$ is nearly linear in $\tilde{x}$ but has a slight convexity towards higher values. The conventional collector boundary condition

is $\underset{\sim}{n}_c \approx 0$, so (17) then gives the relation between the emitter boundary value $\underset{\sim}{n}_e$ and $\underset{\sim}{J}$ as

$$\underset{\sim}{J} = 2\underset{\sim}{n}_e - \ln(1 + \underset{\sim}{n}_e) \tag{18}$$

From equations (11), (13), and (14) the relation between $\underset{\sim}{n}_e$ and $\underset{\sim}{V}$ is

$$\underset{\sim}{n}_p e^{\underset{\sim}{V}} = \underset{\sim}{n}_e(1 + \underset{\sim}{n}_e) \tag{19}$$

so that equations (18) and (19) contain the relation between $\underset{\sim}{J}$ and $\underset{\sim}{V}$ with $\underset{\sim}{n}_e$ as the "emitter injection parameter". Since in these equations one quantity remains which is dependent upon the particular numerical values pertinent to the neutral base region, namely $\underset{\sim}{n}_p \equiv n_p/p_p$, it is convenient to remove this quantity by one further stage of normalization which includes it in the normalized voltage, thus:

$$e^{\underset{\sim}{U}} = \underset{\sim}{n}_e(1 + \underset{\sim}{n}_e) \tag{20}$$

where

$$\underset{\sim}{U} \equiv \underset{\sim}{V} + \ln \underset{\sim}{n}_p \tag{21}$$

Equations (18) and (20) then contain in parametric form the collector current versus base-emitter voltage relation for a transistor of any base material with any conductivity.

The emitter injection parameter $\underset{\sim}{n}_e$ cannot in general be eliminated from equations (18) and (20), but an explicit relation between $\underset{\sim}{J}$ and $\underset{\sim}{U}$ can be obtained for two limiting cases. If $\underset{\sim}{n}_e \ll 1$, the emitter minority carrier density $n_e$ is much less than the equilibrium majority carrier density $p_p$, and the limiting result is

$$\underset{\sim}{J} = e^{\underset{\sim}{U}} \tag{22}$$

This condition is defined as low-level injection at the emitter. If $\underset{\sim}{n}_e \gg 1$, the limiting result is

$$\underset{\sim}{J} = 2\, e^{\underset{\sim}{U}/2} \tag{23}$$

This condition is defined as high-level injection at the emitter.

Physical interpretation of these results is facilitated if it is known what fraction of the total collector current density $J$ is carried by the diffusion component $J_{diff}$. By definition

$$J_{diff} = -eD_n \frac{dn}{dx} = -J_0 \frac{d\underset{\sim}{n}}{d\underset{\sim}{x}} \tag{24}$$

Hence from equation (16),

$$\frac{J_{diff}}{J} = \frac{1 + \underset{\sim}{n}}{1 + 2\underset{\sim}{n}} \tag{25}$$

For low-level injection, $\underset{\sim}{n} \ll 1$ throughout the neutral base region, so the total current is carried essentially entirely by diffusion. Physically, the majority carrier density is everywhere essentially undisturbed, so $V_p$ is very small compared to $V_j$ and the drift component of current is negligible. Hence equation (22) for the total current may be written directly from equations (20) and (24) as

$$\underset{\sim}{J} \approx \underset{\sim}{J}_{diff} = \underset{\sim}{n}_e = e^{\underset{\sim}{U}}$$

For high-level injection, $\underset{\sim}{n} \gg 1$ throughout most of the neutral base, since the distribution of $\underset{\sim}{n}$ with $\underset{\sim}{x}$ is still approximately linear, so from equation (25) about half the total current is carried by diffusion. Physically, the majority and minority carrier densities tend to become equal, so that $V_p$ and $V_j$ become equal, and half the total applied voltage goes to developing an electric field in the neutral base region, which in turn causes the minority carrier drift current to become equal to the diffusion current. Hence equation (23) for the total current may be written directly from equations (20) and (24) as

$$\tilde{J} \approx 2\,\tilde{J}_{diff} = 2\,\tilde{n}_e = 2\,e^{\tilde{U}/2}$$

The low-level and high-level asymptotes given by equations (22) and (23) give straight lines when plotted on semi-log scales, and intersect at a value $\tilde{J} = 4$ as shown in Fig. 2. Since the actual characteristic undergoes a gradual transition from one limiting case to the other in this neighborhood, it is convenient to say that $\tilde{J} \ll 1$ corresponds to low-level injection, and $\tilde{J} \gg 1$ corresponds to high-level injection.

## 2.2. The conventional $\beta$ versus $J$ characteristic

Since $\tilde{n}$ is nearly linear in $\tilde{x}$ at all injection levels, the total injected electron charge $Q$ (per unit area) may be approximated by

$$Q = \frac{1}{2} e(n_e + n_c) w_n = \frac{e p_p w_n}{2} (\tilde{n}_e + \tilde{n}_c) \tag{26}$$

For the conventional collector boundary conditions, $\tilde{n}_c \approx 0$ and $w_n = w_{no}$, and so the injected charge becomes

$$Q = \frac{e p_p w_{no}}{2} \tilde{n}_e \tag{27}$$

The transit time $\tau_t$ of injected electrons across the neutral base region may be defined as

$$\tau_t \equiv \frac{Q}{J} \tag{28}$$

$$= \frac{w_{no}^2}{2D_n} \frac{\underset{\sim}{n}_e}{2\underset{\sim}{n}_e - \ln(1 + \underset{\sim}{n}_e)} \tag{29}$$

from equations (15), (18), and (27). Equation (29) may be written

$$\frac{\tau_{to}}{\tau_t} = 2 - \frac{\ln(1 + \underset{\sim}{n}_e)}{\underset{\sim}{n}_e} \tag{30}$$

where

$$\tau_{to} \equiv \frac{w_{no}^2}{2D_n} \tag{31}$$

is the low-level transit time. For high-level injection the transit time becomes asymptotic to $\tau_{to}/2$ as the drift contribution becomes equal to the diffusion contribution to the total current. With use of equation (18), $\tau_{to}/\tau_t$ may be plotted as a function of normalized current density $\underset{\sim}{J}$ as shown in Fig. 3.

For the simple transistor model under discussion, the emitter efficiency and the collector multiplication factor are each unity since

the emitter and collector conductivities are assumed very high and avalanche multiplication is neglected. Steady-state base current $J_b$ (per unit junction area) therefore arises only from recombination of injected minority carriers in the base region. When recombination within the transition regions is neglected, an "effective lifetime" $\tau_b$ of these minority carriers may be defined by an equation analogous to (25):

$$\tau_b \equiv \frac{Q}{J_b} \tag{32}$$

It follows directly from equations (28) and (32) that the d-c current gain $\beta$ may be expressed as the ratio of the effective lifetime of the injected carriers to their transit time through the neutral base:

$$\beta \equiv \frac{J}{J_b} = \frac{\tau_b}{\tau_t} \tag{33}$$

Since $\tau_t$ as a function of the injection parameter $\underset{\sim}{n}_e$ is known by equation (30), it remains to find a relation between $\tau_b$ and $\underset{\sim}{n}_e$ in order to have an implicit expression for the current gain as a function of collector current.

If surface recombination in the base region is neglected, in line with the one-dimensional model under consideration, volume recombination remains as the sole source of steady-state base current. If recombination

occurs solely through trapping levels in the semiconductor band gap, the lifetime $\tau$ of minority carrier electrons at a point in a charge-neutral semiconductor where the normalized electron density is $\underset{\sim}{n}$ is given by a function of the form[11]

$$\tau = \tau_o \frac{1 + \lambda \underset{\sim}{n}}{1 + \underset{\sim}{n}} \tag{34}$$

where for vanishing injection the lifetime approaches the constant value $\tau_o$. The parameter $\lambda$ is related to the properties of the trapping levels. If recombination occurs solely through direct transitions from the conduction to the valence band, the lifetime is given by a form similar to (34) except that $\lambda = 0$. Either recombination mechanism may therefore be represented by the functional relationship of equation (34).

Since under injection conditions the electron density in the base of an n-p-n transistor is not constant, the lifetime varies across the base. The total base current $J_b$ (due to volume recombination) is the integral of the incremental recombination current density $e(n - n_p)/\tau$ over the base region, and hence the effective lifetime $\tau_b$ may be obtained from equation (32) as

$$\frac{1}{\tau_b} = \int_0^{W_{no}} \frac{e(n - n_p)}{\tau} dx \Bigg/ \int_0^{W_{no}} e(n - n_p) dx$$

In normalized form this becomes

$$\frac{1}{\tau_b} = \int_0^1 \frac{\underset{\sim}{n} - \underset{\sim}{n}_p}{\tau} \, d\underset{\sim}{x} \Bigg/ \int_0^1 (\underset{\sim}{n} - \underset{\sim}{n}_p) d\underset{\sim}{x} \tag{35}$$

Evaluation of equation (35) is considerably simplified if $\underset{\sim}{n}$ is taken to be linear in $\underset{\sim}{x}$, which has already been shown to be a good approximation. Further, $\underset{\sim}{n}_p$ may be omitted for operating currents at which the base and collector saturation currents may be neglected. Under these conditions, equation (35) becomes

$$\frac{1}{\tau_b} = \int_{\underset{\sim}{n}_e}^{\underset{\sim}{n}_c} \frac{1}{\tau} \underset{\sim}{n} \, d\underset{\sim}{n} \Bigg/ \int_{\underset{\sim}{n}_e}^{\underset{\sim}{n}_c} \underset{\sim}{n} \, d\underset{\sim}{n} \tag{36}$$

For the conventional collector boundary value $\underset{\sim}{n}_c = 0$, integration of equation (36) with the functional relation (34) leads to

$$\frac{\tau_o}{\tau_b} = \frac{1}{\lambda} \left[ 1 - \frac{1-\lambda}{\lambda} \frac{2}{\underset{\sim}{n}_e} \left( 1 - \frac{\ln(1 + \lambda \underset{\sim}{n}_e)}{\lambda \underset{\sim}{n}_e} \right) \right] \tag{37}$$

For injection levels low enough that $\lambda \underset{\sim}{n}_e \ll 1$, equation (37) reduces to

$$\frac{\tau_o}{\tau_b} \approx 1 + \frac{2}{3}(1 - \lambda)\underset{\sim}{n}_e \tag{38}$$

and for $\lambda n_{\tilde{e}} \gg 1$ to

$$\frac{\tau_o}{\tau_b} \approx \frac{1}{\lambda}\left(1 - \frac{1-\lambda}{\lambda}\frac{2}{n_{\tilde{e}}}\right) \tag{39}$$

so that $\tau_b$ varies from $\tau_o$ to $\lambda\tau_o$ as the injection level increases. With use of equation (18), $\tau_b/\tau_o$ may be plotted as a function of normalized current $J_{\tilde{}}$ as shown in Fig. 3 for the arbitrary value $\lambda = 0.1$. It may be noted that if $\lambda = 0$ (recombination through direct transitions only), equation (38) is valid for all values of $n_{\tilde{e}}$ and so $\tau_b$ approaches zero instead of levelling off at a finite value as the injection level increases. This case is also shown in Fig. 3.

The current gain $\beta$ may now be obtained from equation (33) as

$$\beta = \frac{\tau_o}{\tau_{to}}\frac{\tau_{to}}{\tau_t}\frac{\tau_b}{\tau_o} = \beta_o \frac{\tau_{to}}{\tau_t}\frac{\tau_b}{\tau_o} \tag{40}$$

where $\beta_o \equiv \tau_o/\tau_{to}$ is the low-injection limit of $\beta$. Substitution from equations (30) and (37) gives $\beta$ as a function of the emitter injection parameter $n_{\tilde{e}}$:

$$\frac{\beta}{\beta_o} = \left[2 - \frac{\ln(1 + n_{\tilde{e}})}{n_{\tilde{e}}}\right]\lambda \Bigg/ \left[1 - \frac{1-\lambda}{\lambda}\frac{2}{n_{\tilde{e}}}\left(1 - \frac{\ln(1 + \lambda n_{\tilde{e}})}{\lambda n_{\tilde{e}}}\right)\right] \tag{41}$$

With use of equation (18), $\beta/\beta_o$ may be plotted as a function of normalized current $\underset{\sim}{J}$ as shown in Fig. 3 for the values $\lambda = 0.1$ and $\lambda = 0$. It is seen that in both cases the decrease in $\tau_b$ at high-level injection more than offsets the increase in $\tau_t$, so $\beta$ decreases monotonically. However, this may not occur if $\lambda$ were larger: in particular, if $\lambda = 1$, $\tau_b/\tau_o = 1$ at all currents and $\beta/\beta_o$ becomes identical with $\tau_{to}/\tau_t$. Also, if finite emitter efficiency were accounted for, the effect of decreasing $\tau_b$ would not become apparent until higher current levels were reached and $\beta$ could show an initial rise even for small values of $\lambda$.

It should be noted that the quantity $\beta$ given by equation (41) is the d-c, not the incremental, current gain, but that the saturation currents have been neglected so that $\beta$ does not go to infinity at zero base current.

## 2.3. Typical numerical values

The foregoing results are in terms of normalized parameters applicable to any device that satisfies the assumptions in the basic model. It is of interest to consider typical numerical values to determine whether or not the parameter ranges displayed in the graphical results correspond to those in practical use.

For illustration, we may consider a germanium n-p-n alloy-junction transistor with base resistivity 2 ohm-cm, metallurgical base thickness 0.9 mil, and circular junctions of diameter 12 mils. The emitter transition region thickness will be negligible for normal forward biases,

and we may suppose that the collector reverse-bias voltage leads to $w_{to} = 0.3$ mil, so that the neutral base thickness is $w_{no} = 0.6$ mil. For 2 ohm-cm p-type germanium at room temperature in which the hole diffusion constant is $D_p = 44$ cm$^2$/sec, the equilibrium carrier densities are $p_p \approx 1.8 \times 10^{15}$ cm$^{-3}$ and $n_p \approx 3.4 \times 10^{11}$ cm$^{-3}$. At room temperature, the normalizing voltage $V_t$ may be taken as 0.025 v.

The most important normalizing parameter is the current density $J_0$, which is found from equation (15) to be $J_0 \approx 18$ amp/cm$^2$ for an electron diffusion constant $D_n = 93$ cm$^2$/sec. A junction diameter of 12 mils corresponds to an area $A = 7.3 \times 10^{-4}$ cm$^2$, so that $\underset{\sim}{J} = 1$ on the current scales of Figs. 2 and 3 corresponds to a total collector current $AJ_0 = 13$ ma. Collector currents considerably higher than this, at least on a pulse basis, could be handled by the illustrative transistor, and we may conclude that high-level injection conditions could occur and that significant drop in current gain from its low-current value could result.

The normalized voltage axis in Fig. 2 may be converted to read actual voltage by use of equation (21). For the assumed typical figures, $\underset{\sim}{n}_p \approx 1.9 \times 10^{-4}$, so for $V_t = 0.025$ v the conversion relation is $V = 0.025(\underset{\sim}{U} + 8.6)$. Hence for $\underset{\sim}{U} = 0$, corresponding approximately to $AJ = AJ_0 = 13$ ma, the forward bias voltage is $V \approx 0.22$ v. If the typical transistor were silicon, instead of germanium, the only significant difference in the normalizing parameters would be that $\underset{\sim}{n}_p$, being about six orders of magnitude smaller, would lead to $V = 0.025(\underset{\sim}{U} + 23.2)$. Hence $\underset{\sim}{U} = 0$ corresponds to $V \approx 0.58$ v.

## 3. The modified collector boundary conditions

In this section the dependences of the collector minority carrier density and transition region thickness upon the current are established. The relations are in forms suitable for use as modified collector boundary conditions in the solution of the neutral base region.

It is shown in a companion paper[3] that the minority carrier density at the edge of the transition region of a reverse-biased p-n junction increases with injected minority carrier current density $J$. As related to the model shown in Fig. 1, this conclusion implies that the boundary value $n_c$ of the electron density is no longer zero. For structures in which the electron velocity in the collector transition region is everywhere less than the limiting drift velocity, $n_c$ increases linearly with $J$ for $n_c < p_p$, and then more slowly as $J^{2/3}$ for $n_c > p_p$. The conditions $n_c \ll p_p$, $n_c \gg p_p$ respectively define low-level and high-level injection at the collector. The collector transition region is essentially depleted of mobile carriers at low-level injection, and is of constant width for a given collector reverse bias. At high-level injection, the transition region becomes an accumulation region of mobile carriers, space-charge-limited minority current is established and the thickness of the transition region decreases with increasing current.

For structures in which the electron velocity in the collector transition region is everywhere equal to the limiting drift velocity $v_m$, $n_c$ increases linearly with $J$ at all injection levels according

to

$$n_c = p_p \frac{J}{J_2} \tag{42}$$

where

$$J_2 \equiv e\mu_n p_p v_m \tag{43}$$

In terms of the injected current, low-level and high-level injection at the collector therefore correspond respectively to $J \ll J_2$, $J \gg J_2$. The transition region thickness is again a depletion region of constant width at low-level injection, and becomes an accumulation region of decreasing width at high-level injection. The relation between the transition region width $w_t$ and its value $w_{to}$ at low-level injection is given in terms of $n_c$ by

$$w_t = \frac{w_{to}}{(1 + n_c/p_p)^{1/2}} \tag{44}$$

For most transistors, and in particular for alloy junction types, conditions are such that the minority carrier velocity is essentially equal to the limiting drift velocity throughout the collector transition region, and so the modified boundary conditions for this case only will

be considered.

Since both the position of the collector boundary of the base region, and the value of the minority carrier density at that boundary, differ from the conventional results, it is clear that changes in the basic solution of the transistor properties will occur when the modified collector boundary conditions are taken into account. Three conditions of operation may be distinguished. In Condition I, $n_e \ll p_p$, $n_c \ll p_p$; in Condition II, $n_e \gg p_p$, $n_c \ll p_p$; and in Condition III, $n_e \gg p_p$, $n_c \gg p_p$. The carrier density distributions for these three conditions are indicated in Fig. 4, in which the density scales are again distorted to emphasize the salient features of the distributions. Conditions I and II correspond respectively to low-level and to high-level injection at the emitter; in Condition III high-level injection into the collector transition region occurs and the effective neutral base thickness $w_n$ increases with current.

In normalized form, equation (42) is

$$\underset{\sim}{n}_c = \theta \underset{\sim}{J} \tag{45}$$

where

$$\theta \equiv \frac{J_0}{J_2} = \frac{D_n}{v_m w_{no}} \tag{46}$$

by equations (15) and (46). The value $\theta = 0.01$ is obtained for the typical germanium alloy-junction transistor discussed in section 2.3, if the limiting drift velocity for electrons is taken to be $v_m = 6 \times 10^6$ cm/sec. In any case, $\theta$ is always much less than unity.

Equation (44) is more conveniently expressed in terms of the neutral base width $w_n$ rather than in terms of $w_t$, thus

$$\frac{w_n}{w_{no}} = \frac{w - w_t}{w_{no}} = 1 + \frac{w_{to} - w_t}{w_{no}}$$

$$= 1 + \phi \left( 1 - \frac{1}{\sqrt{1+n_{\sim c}}} \right) \tag{47}$$

where

$$\phi \equiv \frac{w_{to}}{w_{no}} \tag{48}$$

The value $\phi = 0.5$ is obtained for the same typical transistor indicating that at zero current, and at a given collector reverse bias voltage, the collector depletion layer penetrates one-third of the base p-region.

Equations (45) and (47) constitute the modified collector boundary conditions to be used in the solution of the neutral base region.

## 4. Solution with modified collector boundary conditions

We now consider the modifications in the basic characteristics of a transistor that are to be expected when modified collector boundary conditions are employed.

### 4.1. The modified J versus V characteristic

The quantitative effects of the modified collector boundary conditions may be determined by retracing the steps followed in section 2 for the conventional solution. The first change required is that since distance $x$ through the neutral base region must now be normalized to $w_n$, instead of to $w_{no}$, so that $\underset{\sim}{x} \equiv x/w_n$, the basic differential equation for $\underset{\sim}{n}$ is modified from the expression (16) to

$$\frac{1 + 2\underset{\sim}{n}}{1 + \underset{\sim}{n}} \frac{d\underset{\sim}{n}}{d\underset{\sim}{x}} = - \underset{\sim}{J} \frac{w_n}{w_{no}} = - \underset{\sim}{J} \left[ 1 + \phi f_1(\underset{\sim}{n}_c) \right] \tag{49}$$

where the function $f_1(\eta)$ is defined by

$$f_1(\eta) \equiv 1 - \frac{1}{\sqrt{1+\eta}} \tag{50}$$

from equation (47). The solution of equation (49) is

$$2\underset{\sim}{n} - \ln(1+\underset{\sim}{n}) = \underset{\sim}{J} \left[ 1 + \phi f_1(\underset{\sim}{n}_c) \right] (1-\underset{\sim}{x}) + 2\underset{\sim}{n}_c - \ln(1+\underset{\sim}{n}_c) \tag{51}$$

and so $\underset{\sim}{n}$ is again nearly linear in $\underset{\sim}{x}$. With insertion of the emitter boundary value $\underset{\sim}{n} = \underset{\sim}{n}_e$ at $\underset{\sim}{x} = 0$, equation (51) leads to

$$\underset{\sim}{J} = \frac{\underset{\sim}{n}_e f_2(\underset{\sim}{n}_e) - \underset{\sim}{n}_c f_2(\underset{\sim}{n}_c)}{1 + \phi f_1(\underset{\sim}{n}_c)} \tag{52}$$

where

$$f_2(\eta) \equiv 2 - \frac{\ln(1+\eta)}{\eta} \tag{53}$$

The functions $f_1(\eta)$ and $f_2(\eta)$ are plotted in Fig. 5, where it is seen that both functions approach asymptotic values both for very small $\eta$ and for very large $\eta$, with $\eta \approx 1$ defining approximately the transition from one asymptotic value to the other.

Since $\underset{\sim}{n}_c = \theta \underset{\sim}{J}$ by (45), equation (52) implies a unique relationship between the emitter injection parameter $\underset{\sim}{n}_e$ and the collector current $\underset{\sim}{J}$. Rearrangement of equation (52) gives

$$\frac{\underset{\sim}{n}_e}{\underset{\sim}{J}} f_2(\underset{\sim}{n}_e) = 1 + \phi f_1(\theta \underset{\sim}{J}) + \theta f_2(\theta \underset{\sim}{J}) \tag{54}$$

so that with use of Fig. 5 $\underset{\sim}{n}_e$ may be plotted as a function of $\underset{\sim}{J}$. Since $\underset{\sim}{n}_e$ increases rapidly with $\underset{\sim}{J}$, it is more convenient to plot the quantity

$$F \equiv \frac{n_{\sim e}}{J_{\sim}} = \theta \frac{n_{\sim e}}{n_{\sim c}} \tag{55}$$

rather than $n_{\sim e}$ as a function of $J_{\sim}$, since $F$ approaches a limiting value at high injection and a more expanded scale may be used. The function $F(J)$ is plotted in Fig. 6 for the typical parameter values $\theta = 0.01$, $\phi = 0.5$. It may be noted that the plot of $F$ also represents the ratio $n_{\sim e}/n_{\sim c}$ as a function of $J_{\sim}$ when multiplied by the scale factor $1/\theta$.

Three asymptotic forms of equation (54), and therefore of equation (55), may be distinguished, which correspond to the three injection conditions.

Condition I: $n_{\sim e} \ll 1$, $n_{\sim c} = \theta J_{\sim} \ll 1$

$$F = \frac{n_{\sim e}}{J_{\sim}} \approx 1+\theta, \qquad \frac{n_{\sim c}}{n_{\sim e}} = \frac{\theta}{F} \approx \frac{\theta}{1+\theta} \tag{56}$$

Condition II: $n_{\sim e} \gg 1$, $n_{\sim c} = \theta J_{\sim} \ll 1$

$$F = \frac{n_{\sim e}}{J_{\sim}} \approx \frac{1+\theta}{2}, \qquad \frac{n_{\sim c}}{n_{\sim e}} = \frac{\theta}{F} \approx \frac{2\theta}{1+\theta} \tag{57}$$

Condition III: $n_{\sim e} \gg 1$, $n_{\sim c} = \theta J_{\sim} \gg 1$

$$F = \frac{n_{\sim e}}{J_{\sim}} \approx \frac{1+2\theta+\phi}{2}, \qquad \frac{n_{\sim c}}{n_{\sim e}} = \frac{\theta}{F} \approx \frac{2\theta}{1+2\theta+\phi} \tag{58}$$

These asymptotes are also shown in Fig. 6. It may be noted that F varies over only a small range of values, and that $\underset{\sim}{n}_c$ is always much less than $\underset{\sim}{n}_e$.

The relation between the normalized base-emitter voltage $\underset{\sim}{V}$ and the emitter injection parameter $\underset{\sim}{n}_e$ is unaffected by the modified collector boundary conditions, and remains

$$e^{\underset{\sim}{U}} = \underset{\sim}{n}_e(1 + \underset{\sim}{n}_e) \tag{59}$$

as in equation (20). Equations (58) and (59) therefore define the transistor transfer characteristic including the modified collector boundary conditions. With use of Fig. 6, a numerical plot of $\underset{\sim}{J}$ versus $\underset{\sim}{U}$ can be obtained, as shown in Fig. 2 for the typical parameter values $\theta = 0.01$, $\phi = 0.5$. Only two asymptotic forms of equation (59) occur:

Condition I:

$$e^{\underset{\sim}{U}} \approx \underset{\sim}{n}_e \tag{60}$$

Conditions II and III:

$$e^{\underset{\sim}{U}} \approx n_e^2 \tag{61}$$

The salient features of the complete transfer characteristic may be seen by combining the appropriate asymptotic forms of equations (54) and (59):

Condition I, from equations (56) and (60):

$$\underset{\sim}{J} = \frac{1}{1+\theta} e^{\underset{\sim}{U}} \tag{62}$$

Condition II, from equations (57) and (61):

$$\underset{\sim}{J} = \frac{2}{1+\theta} e^{\underset{\sim}{U}/2} \tag{63}$$

Condition III, from equations (58) and (61):

$$\underset{\sim}{J} = \frac{2}{1+2\theta+\phi} e^{\underset{\sim}{U}/2} \tag{64}$$

It is apparent that little departure from the conventional case occurs in Conditions I and II, since equations (62) and (63) are the same as equations (22) and (23) except for the factor $(1+\theta) = 1.01$ which, as shown in Fig. 2, displaces the asymptotes by a negligible amount. On the other hand, equation (64) represents a significant departure from the corresponding result for the conventional case, equation (23), as shown in Fig. 2 for $\phi = 0.5$. Cross-over between Conditions I and II

occurs at $\underset{\sim}{n}_e = 1$ or $\underset{\sim}{J} \approx 1$; cross-over between Conditions II and III occurs at $\underset{\sim}{n}_c = 1$ or $\underset{\sim}{J} \approx 1/\theta$.

We may conclude that the modified collector boundary value has negligible effect on the collector current versus base-emitter voltage transfer characteristic. However, the modified collector boundary position can introduce a significant decrease in the collector current at a given base-emitter voltage when the current is high enough that high-level injection into the collector transition region takes place.

## 4.2. The modified $\beta$ versus $J$ characteristic

The effects of the modified collector boundary conditions on the current gain $\beta$ are somewhat more complex than are those on the transfer characteristic, and may be investigated by introducing appropriate corrections to the conventional treatment.

From equations (15), (26) and (31) the total injected electron charge into the neutral base region is given by

$$Q = \tau_{to} J_0 \left[1+\phi f_1(\underset{\sim}{n}_c)\right](\underset{\sim}{n}_e + \underset{\sim}{n}_c) \tag{65}$$

From equations (28) and (65), the transit time is then given by

$$\frac{\tau_{to}}{\tau_t} = \tau_{to} J_0 \frac{\underset{\sim}{J}}{Q} = \frac{\underset{\sim}{J}}{[1+\phi f_1(\underset{\sim}{n}_c)](\underset{\sim}{n}_e + \underset{\sim}{n}_c)} \tag{66}$$

$$= \frac{\underset{\sim}{n}_e f_2(\underset{\sim}{n}_e) - \underset{\sim}{n}_c f_2(\underset{\sim}{n}_c)}{[1+\phi f_1(\underset{\sim}{n}_c)]^2 (\underset{\sim}{n}_e + \underset{\sim}{n}_c)} \tag{67}$$

by equation (52). Equation (67) is a formal expression for the normalized transit time in terms of the emitter and collector boundary values, but since $\underset{\sim}{n}_e$ and $\underset{\sim}{n}_c$ are both unique functions of $\underset{\sim}{J}$ it is more convenient to modify equation (66) in order to plot $\tau_{to}/\tau_t$ versus $\underset{\sim}{J}$. With use of $\underset{\sim}{n}_c = \theta \underset{\sim}{J}$ and equation (55), equation (66) becomes

$$\frac{\tau_{to}}{\tau_t} = \frac{1}{[1+\phi f_1(\theta \underset{\sim}{J})](F + \theta)} \tag{68}$$

With use of Figs. 5 and 6, equation (68) may be plotted as a function of $\underset{\sim}{J}$ as shown in Fig. 7 for the typical values $\theta = 0.01$, $\phi = 0.5$. Asymptotic forms of equation (67) or (68) for the three injection conditions are easily obtained.

Condition I:

$$\frac{\tau_{to}}{\tau_t} \approx \frac{1}{1+2\theta} \tag{69}$$

Condition II:

$$\frac{\tau_{to}}{\tau_t} \approx \frac{2}{1+3\theta} \tag{70}$$

Condition III:

$$\frac{\tau_{to}}{\tau_t} \approx \frac{2}{(1+4\theta+\phi)(1+\phi)} \tag{71}$$

The results for Conditions I and II indicate little deviation from those for the conventional case, but in Condition III the transit time is larger than in the conventional case by a factor approximately $(1+\phi)^2$. Physically, we conclude that the modified collector boundary value again has little effect on the results but that the increased neutral base thickness at high-level injection into the collector transition region leads to significant increase in the transit time. Since the transit time is proportional to the square of the relevant distance, the factor $(1+\phi)^2$ in Condition III is to be expected.

The expression for the effective lifetime due to volume recombination in the neutral base remains as in equation (36), where the same assumptions and approximations are made. Integration of equation (36), with retention of the finite collector boundary value $\underset{\sim}{n}_c$, gives

$$\frac{\tau_o}{\tau_b} = \frac{1}{\lambda}\left[1 - \frac{1-\lambda}{\lambda}\frac{2}{\underset{\sim}{n}_e + \underset{\sim}{n}_c}\left(1 - \frac{\ln(1+\lambda\underset{\sim}{n}_e) - \ln(1+\lambda\underset{\sim}{n}_c)}{\lambda(\underset{\sim}{n}_e - \underset{\sim}{n}_c)}\right)\right] \tag{72}$$

For injection levels low enough that $\lambda\underset{\sim}{n}_e \ll 1$, equation (72) reduces

to

$$\frac{\tau_o}{\tau_b} \approx 1 + \frac{2}{3}(1-\lambda)\left( \underset{\sim}{n}_e + \frac{\underset{\sim}{n}_c^{\,2}}{\underset{\sim}{n}_e - \underset{\sim}{n}_c} \right) \tag{73}$$

and for $\lambda \underset{\sim}{n}_e \gg 1$ to

$$\frac{\tau_o}{\tau_b} \approx \frac{1}{\lambda}\left( 1 + \frac{1-\lambda}{\lambda} \frac{2}{\underset{\sim}{n}_e + \underset{\sim}{n}_c} \right) \tag{74}$$

so that $\tau_b$ varies from $\tau_o$ to $\lambda\tau_o$ as the injection level increases just as in the conventional case, and between these limits $\tau_o/\tau_b$ is negligibly different from the result in the conventional case. Equation (72) is more conveniently expressed as a function of $\underset{\sim}{J}$ by use of $\underset{\sim}{n}_c = \theta \underset{\sim}{J}$ and equation (55):

$$\frac{\tau_o}{\tau_b} = \frac{1}{\lambda}\left[ 1 - \frac{1-\lambda}{\lambda \underset{\sim}{J}} \frac{2}{F+\theta}\left( 1 - \frac{\ln(1+\lambda F \underset{\sim}{J}) - \ln(1+\lambda\theta\underset{\sim}{J})}{\lambda \underset{\sim}{J}(F-\theta)} \right) \right] \tag{75}$$

The ratio $\tau_o/\tau_b$ is plotted in Fig. 7 as a function of $\underset{\sim}{J}$ by use of Fig. 6, again for the typical values $\theta = 0.01$, $\phi = 0.5$, and for the two values $\lambda = 0$, $\lambda = 0.1$.

Finally, the current gain $\beta$ may be found from

$$\frac{\beta}{\beta_o} = \frac{\tau_{to}}{\tau_t} \frac{\tau_b}{\tau_o} \tag{76}$$

and can be evaluated from the product of equations (68) and (75). The normalized current gain $\beta/\beta_o$ is plotted as a function of $\underset{\sim}{J}$ in Fig. 7 for the typical values $\theta = 0.01$, $\phi = 0.5$, and for $\lambda = 0.1$ and $\lambda = 0$. It is seen that there is little difference from the result shown in Fig. 3 for the conventional case, and that the most significant departure occurs at current levels already so high that the current gain is much less than its low-injection value.

We thus conclude that the d-c current gain is negligibly affected by the modified collector boundary value, and that the comparatively small effects due to the modified collector boundary position are not evident until the current gain has fallen well below its low-injection value.

## 5. Validity of the charge neutrality assumption

It has been shown by Matz[2] that the conventional solution for the minority carrier distribution in the transistor base region, in which the collector boundary value is taken as zero, violates the initial assumption of charge neutrality under high-level injection conditions. It will be shown in this section that use of the modified collector boundary conditions removes this difficulty, and that the initial assumption of a substantially charge-neutral base region is indeed valid.

The argument consists in showing that the curvature in potential predicted on the assumption of charge neutrality implies, through Poisson's equation, an unneutralized charge density which is small compared to the majority carrier charge density at any point within

the assumed charge-neutral base region and at any injection level. From equations (9) and (10), the electric field $-d\underset{\sim}{V}/d\underset{\sim}{x}$ is

$$\frac{d\underset{\sim}{V}}{d\underset{\sim}{x}} = - \frac{1}{1 + \underset{\sim}{n}} \frac{d\underset{\sim}{n}}{d\underset{\sim}{x}} = \frac{\underset{\sim}{J}}{1 + 2\underset{\sim}{n}} \tag{77}$$

from equation (16). Differentiation with respect to $\underset{\sim}{x}$ then gives

$$\frac{d^2\underset{\sim}{V}}{d\underset{\sim}{x}^2} = - \frac{2\underset{\sim}{J}}{(1 + 2\underset{\sim}{n})^2} \frac{d\underset{\sim}{n}}{d\underset{\sim}{x}} = 2\underset{\sim}{J}^2 \frac{1 + \underset{\sim}{n}}{(1 + 2\underset{\sim}{n})^3} \tag{78}$$

Poisson's equation is

$$\frac{d^2V}{dx^2} = - \frac{en_u}{\epsilon} \tag{79}$$

where $en_u$ is the effective unneutralized (positive) charge density. In normalized form, equation (79) is

$$\frac{d^2\underset{\sim}{V}}{d\underset{\sim}{x}^2} = -\left(\frac{w_n}{L_D}\right)^2 \underset{\sim}{n}_u \tag{80}$$

where the unneutralized charge density is normalized to $p_p$, so that $\underset{\sim}{n}_u \equiv n_u/p_p$, and

$$L_D \equiv \sqrt{\frac{\epsilon V_t}{eN_A}} \tag{81}$$

is the Debye length characteristic of p-type material sufficiently extrinsic that $p_p \approx N_A$. From equations (78) and (80),

$$\underset{\sim}{n}_u = - \underset{\sim}{J}^2 \left( \frac{\sqrt{2} L_D}{w_n} \right)^2 \frac{1 + \underset{\sim}{n}}{(1 + 2\underset{\sim}{n})^3} \tag{82}$$

The original charge neutrality assumption is valid if $|n_u|$ is much less than the majority carrier density $p$, or if the ratio $u \equiv |\underset{\sim}{n}_u|/(1+\underset{\sim}{n})$ is much less than unity. Hence the critical quantity is

$$u = \frac{\underset{\sim}{J}^2}{(1 + 2\underset{\sim}{n})^3} \left( \frac{\sqrt{2} L_D}{w_n} \right)^2 \tag{83}$$

For a given current, the largest value $u = u_c$ occurs when $\underset{\sim}{n}$ is smallest, which is at the collector boundary of the neutral base region where $\underset{\sim}{n} = \underset{\sim}{n}_c$. For the conventional boundary conditions, $\underset{\sim}{n}_c = 0$ and $w_n = w_{no}$ so that

$$u_c = \underset{\sim}{J}^2 \left( \frac{\sqrt{2} L_D}{w_{no}} \right)^2 \tag{84}$$

$$= (10^{-2}\underset{\sim}{J}^2)^2$$

for the typical figures specified in section 2.3. Hence for sufficiently large currents $n_c$ can approach and exceed unity, and the charge neutrality assumption breaks down.

For the modified collector boundary conditions, $\underset{\sim}{n}_c = \theta\underset{\sim}{J}$ and $w_n = w_{no}[1+\phi f_1(\theta\underset{\sim}{J})]$, so that

$$u_c = \frac{\underset{\sim}{J}^2}{(1 + 2\theta\underset{\sim}{J})^3}\left(\frac{\sqrt{2}L_D}{w_{no}}\right)^2 \frac{1}{[1+\phi f_1(\theta\underset{\sim}{J})]^2} \qquad (85)$$

The factor $\underset{\sim}{J}^2/(1+2\theta\underset{\sim}{J})^3$ attains a maximum value of $1/27\theta^2$ at $\underset{\sim}{J} = 1/\theta$, and hence since the factor $[1+\phi f_1(\theta\underset{\sim}{J})]$ varies over only a small range, $u_c$ is always less than a maximum value $u_{cm}$ given by

$$u_{cm} = \frac{1}{27}\left(\frac{\sqrt{2}L_D}{\theta w_{no}}\right)^2 = \frac{1}{27}\left(\frac{\sqrt{2}v_m L_D}{D_n}\right)^2 \qquad (86)$$

where the second form is obtained from equation (46). It may be noted that $u_{cm}$ is independent of the device geometry. For the typical figures specified in section 2.3,

$$u_{cm} = \frac{1}{27} = 0.037$$

The unneutralized charge density therefore does not exceed 3.7% of the majority carrier density under any injection conditions, and the initial assumption of charge neutrality is thus justified when the modified collector boundary conditions are taken into account. It may be seen from equation (85) that the assumption is even better at injection levels both higher and lower than that which corresponds to the worst-case condition $\underset{\sim}{n}_c = 1$.

## 6. Conclusions

The basic solution for the minority carrier density distribution in the base region of an n-p-n alloy-junction transistor has been presented. The particular terminal properties derived are the collector current $J$ versus base-emitter voltage $V$ transfer characteristic, and the d-c current gain $\beta$ versus collector current $J$.

In the conventional solution, reviewed in section 2, a collector transition region, essentially completely depleted of mobile carriers, is assumed to extend a precise distance into an otherwise charge-neutral base region. The transition region thickness, and hence the neutral base thickness $W_n$, is a function only of the collector reverse-bias voltage; the minority carrier electron density $n_c$ at the base side of the transition region is related to the equilibrium density by a simple Boltzmann factor, which is essentially zero for normal reverse biases. Zero density at a fixed distance $W_n$ from the emitter junction constitute the conventional collector boundary conditions in the solution

of the minority carrier distribution in the neutral base region. The first-order solution, with neglect of recombination, leads to the J versus V transfer characteristic. Two asymptotic forms are obtained: for low-level injection at the emitter junction, J increases exponentially with V; for high-level injection at the emitter, J increases exponentially with V/2. The base current $J_b$, and hence the current gain $\beta$, is calculated as second-order perturbation by integrating the recombination current required by the first-order minority carrier distribution in the neutral base. The assumed functional dependence of lifetime on minority carrier density allows for recombination both through traps and through direct transitions. It is found that at high-level injection $\beta$ falls considerably below its low injection value.

Two of the basic assumptions in the conventional solution are untenable. Zero minority carrier density would require infinite carrier velocity at any non-zero collector current, and the neutrality assumption in the "neutral" base region is violated at high-level injection. It is shown in a companion paper that reconsideration of conditions in the collector transition region leads to a value of $n_c$ that increases with current, and to a decrease in transition region thickness, together with carrier accumulation instead of depletion, at high-level injection into the collector transition region. The particular case where the carrier velocity in the transition region is saturated at the limiting drift velocity is summarized in section 3. The value of the minority carrier density $n_c$ and its distance $w_n$ from the emitter, both now functions of J, constitute modified collector

boundary conditions.

In the solution for the minority carrier distribution in the presence of the modified collector boundary conditions, discussed in detail in section 4, three regions of operation are distinguished. Condition I corresponds to low-level injection at both emitter and collector; Condition II to high-level injection at the emitter, low-level at the collector; and Condition III to high-level injection at both emitter and collector. The transition from Condition I to Condition II corresponds to that between low-level and high-level injection in the conventional case, and the transition from Condition II to Condition III occurs at a current level about two orders of magnitude higher than that corresponding to the first transition. It is shown that the modified collector boundary value has a negligible effect upon either the $J$ versus $V$ transfer characteristic or the $\beta$ versus $J$ characteristic, but that the modified boundary position can exert a significant effect in the Condition III region. Use of the modified collector boundary conditions eliminates the violation of the charge-neutrality assumption, as shown in section 5, and therefore both major objections to the conventional solution are removed.

It must be recognized that the model upon which both the conventional and the modified solutions are based is highly idealized. It is to be expected, therefore, that the comparatively small differences between the characteristics predicted by the two solutions would be completely masked in practical devices by deviations due to many other effects not included in the analysis. This is particularly likely at high current levels.

The deviations produced by modified collector boundary conditions of the other limiting case discussed in section 3, in which the boundary value and its position are both more slowly varying functions of current, would clearly be of even less significance. It is, in fact, reassuring that essentially unobservable modifications to the conventional solution are predicted, since any significant discrepancies would surely have been detected long ago.

It may be concluded, therefore, that the modified collector boundary conditions serve a useful purpose in that the two major objections to the conventional assumptions are satisfactorily removed, and that we may continue to use the conventional theory and results with confidence that they do, in fact, predict quite closely the performance to be expected -- at least within the limitations of the model.

## Acknowledgements

Valuable discussions with and assistance from M-A. Nicolet and G. W. Lewicki are gratefully acknowledged. The work was supported in part by funds made available by the Jet Propulsion Laboratory of the California Institute of Technology from NASA Contract No. NAS 7-100.

References


1. W. Shockley, Bell Syst. Tech. J., 28, 435, (1949).

2. A. W. Matz, J. Electronics and Control, 7, 133, (1959).

3. R. D. Middlebrook, Solid-State Electronics,

4. C. T. Kirk, I.R.E. Trans. on Electron Devices, ED-9, 164, (1962).

5. R. Beaufoy and J. J. Sparkes, A.T.E. Journal, 13, 310, (1957).

6. E. O. Johnson and A. Rose, Proc. I.R.E., 47, 407, (1959).

7. W. M. Webster, Proc. I.R.E., 42, 914, (1954).

8. R. D. Middlebrook, Proc. I.E.E., 106, Part B, Supplement No. 17, 887, (1959).

9. L. J. Varnerin, Proc. I.R.E., 47, 523, (1959).

10. M. B. Das and A. R. Boothroyd, I.R.E. Trans. on Electron Devices, ED-8, 15, (1961).

11. W. Shockley and W. T. Read, Phys. Rev., 87, 835, (1952).

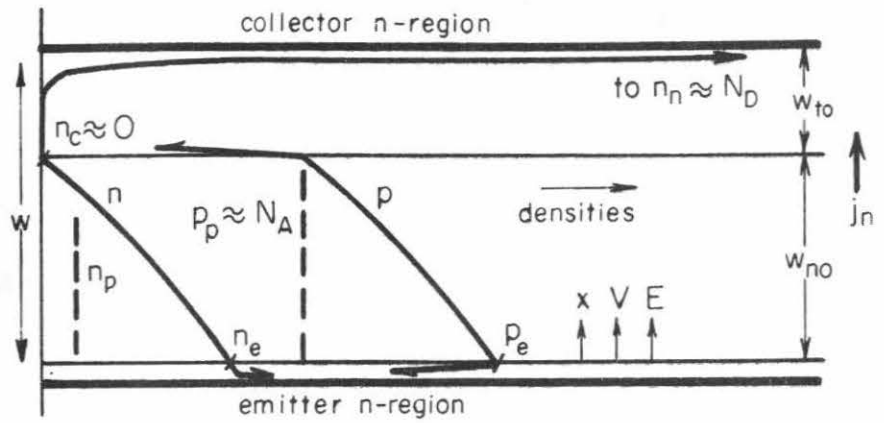


Fig. 1. Model of an n-p-n alloy junction transistor. The base p-region is assumed to be uniformly doped. Carrier densities are indicated for forward-biased emitter, reverse-biased collector. Conventional collector boundary conditions are shown, for which $n_c \approx 0$ and $w_{to}$ is independent of current.

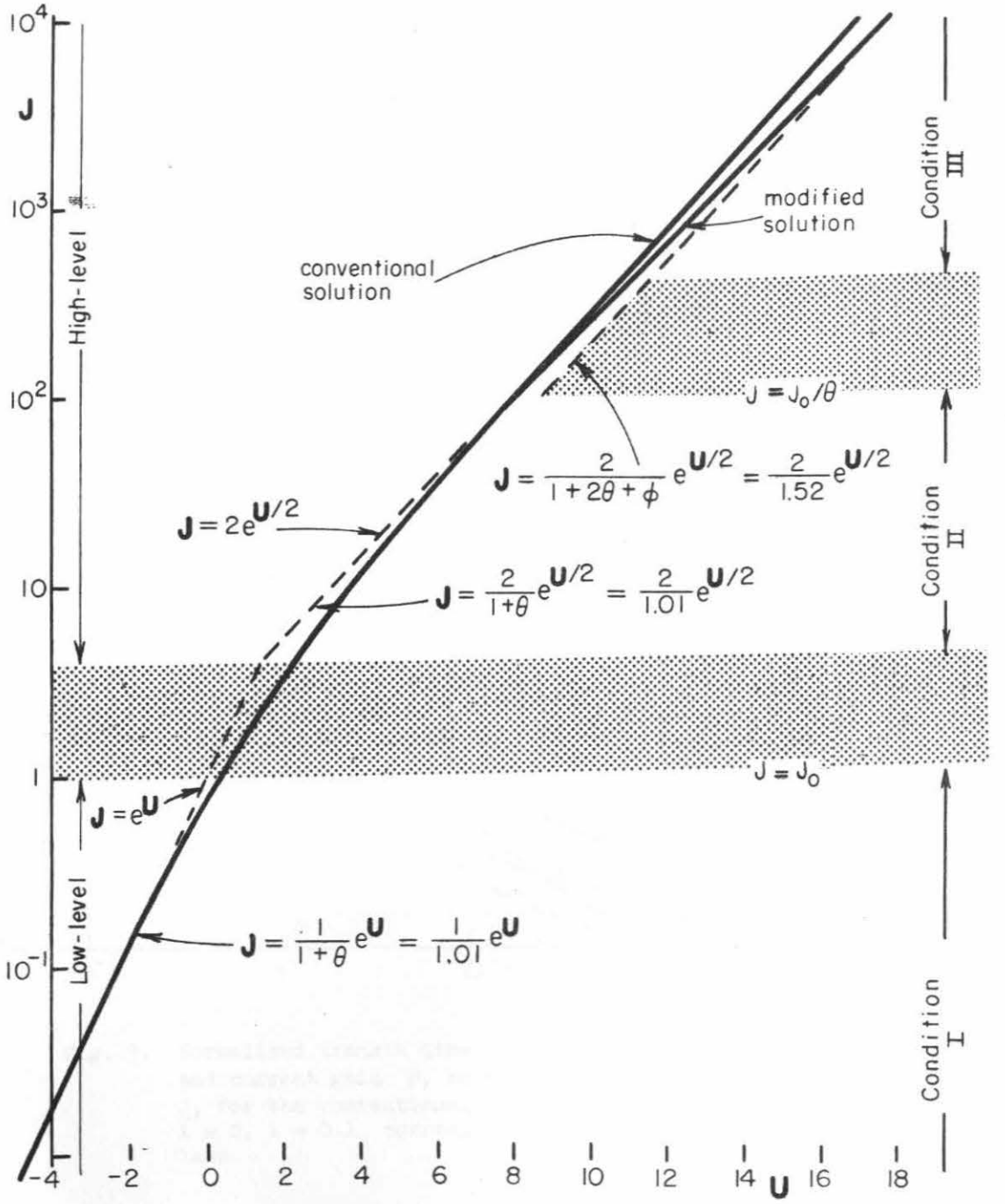


Fig. 2. Normalized collector current $\underset{\sim}{J}$ versus base-emitter voltage $\underset{\sim}{U}$ transfer characteristic. For the conventional solution, two asymptotic forms are obtained; for the modified solution, three asymptotic forms are obtained, of which only that for Condition III differs significantly from the conventional solution.

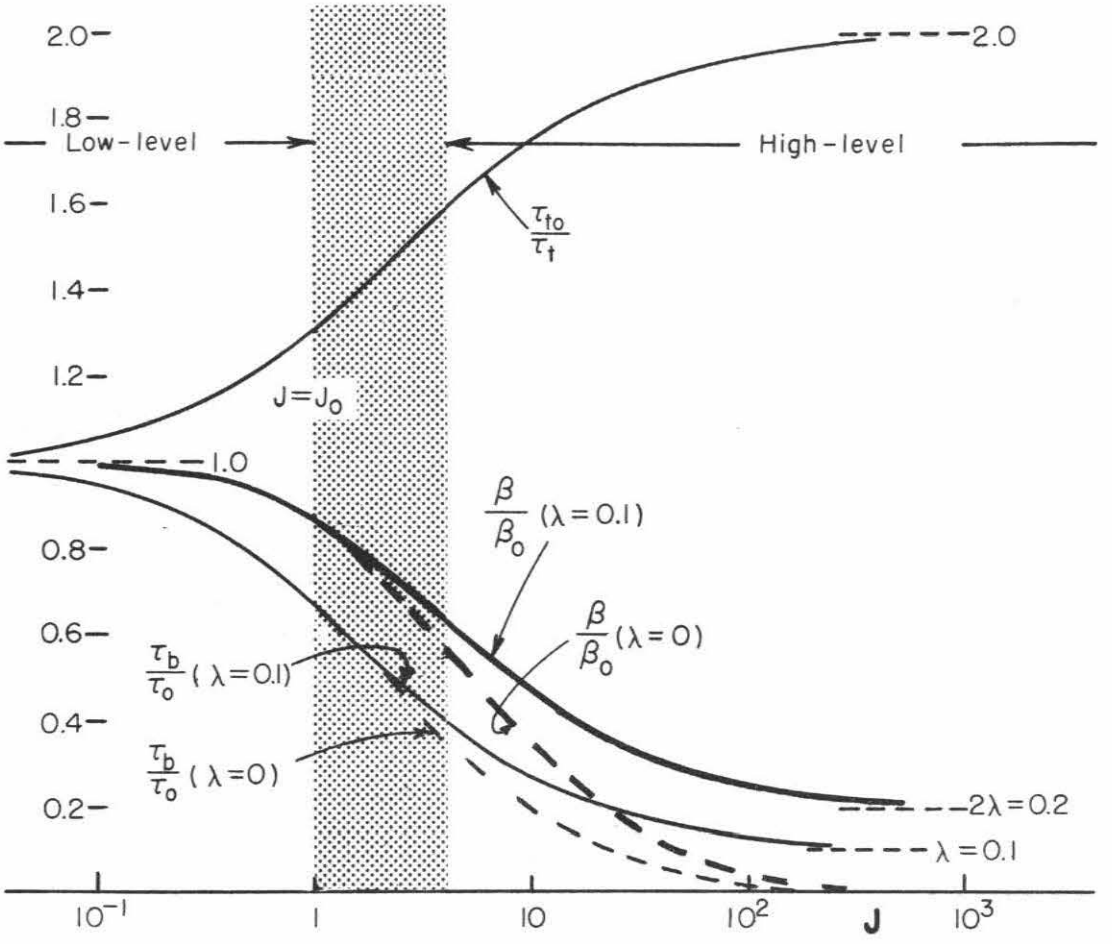


Fig. 3. Normalized transit time $\tau_t$, effective lifetime $\tau_b$, and current gain $\beta$, as functions of normalized current J, for the conventional solution. The parameter values $\lambda = 0$, $\lambda = 0.1$ correspond to two different recombination laws.

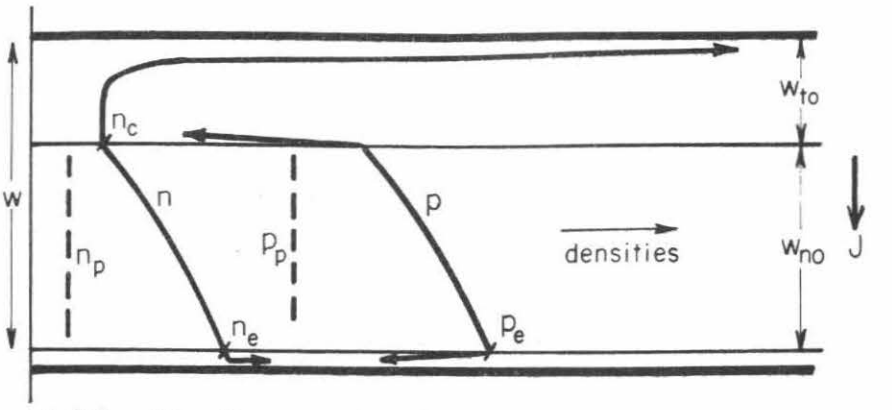


(a) Condition I: $n_e \ll p_p$ , $n_c \ll p_p$

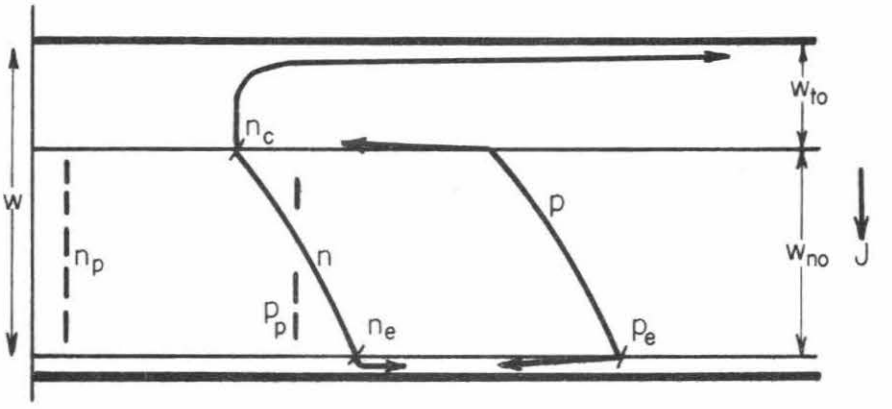


(b) Condition II: $n_e \gg p_p$ , $n_c \ll p_p$

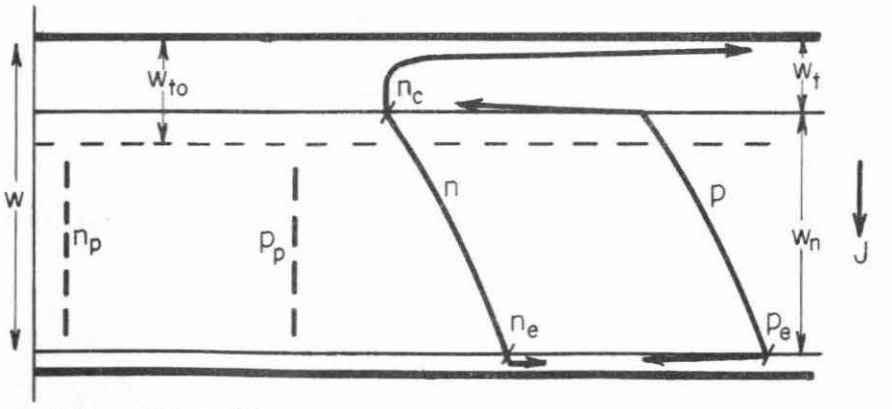


(c) Condition III: $n_e \gg p_p$ , $n_c \gg p_p$

Fig. 4. Carrier densities for the modified collector boundary conditions. Three cases are distinguished.

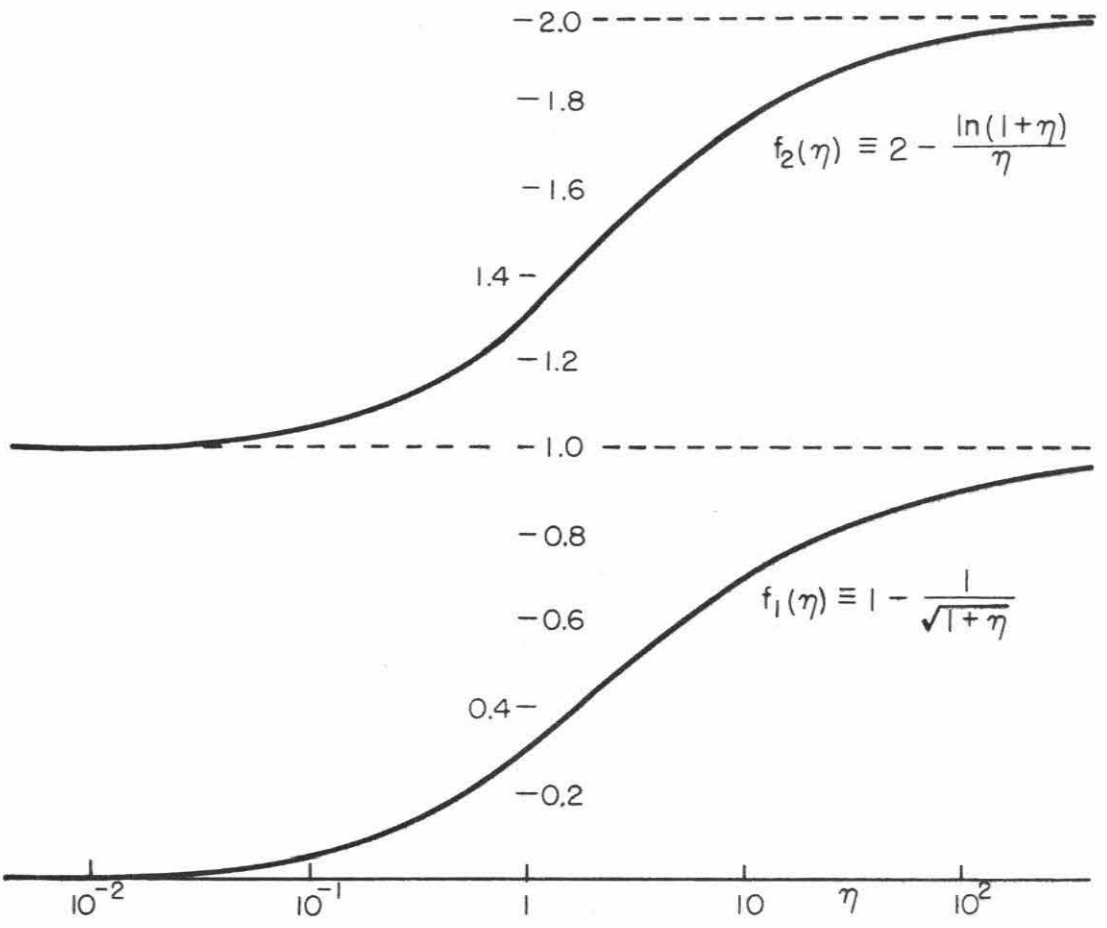


Fig. 5. Plots of the functions $f_1(\eta)$ and $f_2(\eta)$.

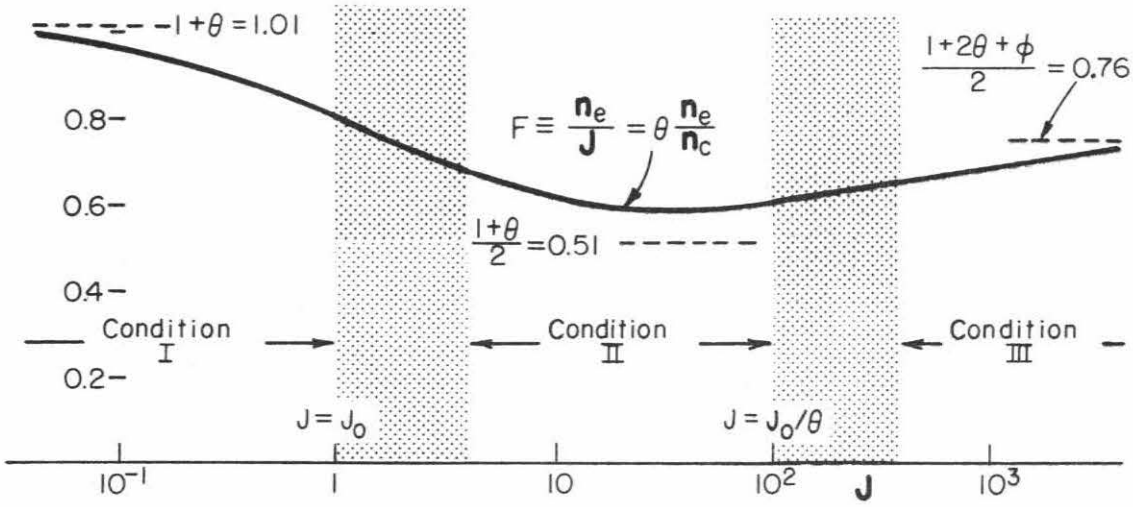


Fig. 6. Plot of the function $F(J)$. Three asymptotic forms are obtained.

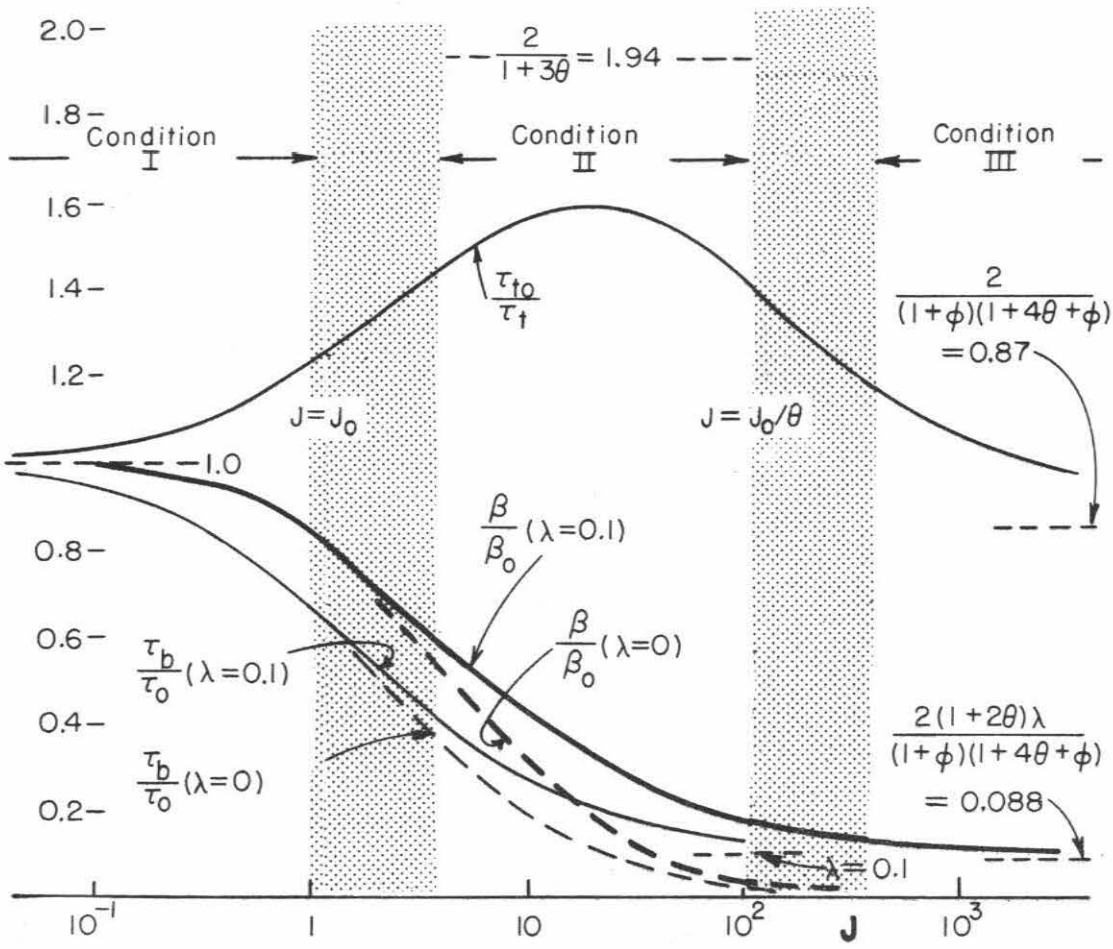


Fig. 7. Normalized transit time $\tau_t$, effective lifetime $\tau_b$, and current gain $\beta$, as functions of normalized current $J$, for the modified solution. Significant deviation from the conventional solution is apparent only in the transit time variation.